Supporting information

Potent and selective A_3 adenosine receptor antagonists bearing aminoesters as heterobifunctional moieties

Stephanie Federico et al.

Experimental

Chemistry

General. All the performed reactions were monitored by silica gel thin-layer chromatography (precoated Macherey-Nagel, 60FUV254). Macherey-Nagel, silica 60, 230-400 mesh silica gel was used to perform flash chromatography purification. Buchi-Tottoli instrument was used to determine compounds melting points and are uncorrected. ^{1}H-NMR spectra were recorded with a Varian Gemini 200 and samples were dissolved in $CDCl_3$ solutions. J values are given in Hz. Accurate mass spectra were recorded on a micrOTOF-Q-Bruker using methanol as solvent to dissolve compounds.
Procedures for the obtainment of compound **15** were previously reported.[1]

General procedure for the synthesis of the 5-aminoesters-2-furan-2-yl-8-methyl-8*H*-pyrazolo[4,3-*e*][1,2,4]triazolo[1,5-*c*]pyrimidine (1-14). 5-Chloro-derivative **15** (100 mg, 0.364 mmol) was dissolved in 5 mL of ethanol (methanol for the synthesis of compound **13**) in a tube. Triethylamine (1.092 mmol, 152 µL) and the appropriate aminoacid ethyl ester (1.092 mmol) were added to the mixture, the tube was sealed and heated at 110°C for 2 hours. The reaction was monitored through thin layer chromatography (EtOAc 9 : MeOH 1). The solvent was then removed under reduced pressure and the residue purified by column cromatography (EtOAc 9.5 : MeOH 0.5) affording the desired compounds (**1-14**).

2-(2-Furan-2-yl-8-methyl-8H-pyrazolo[4,3-e][1,2,4]triazolo[1,5-c]pyrimidin-5-ylamino)-propanoic acid ethyl ester (**1**): yield 35%; yellow solid; mp 55°C ^{1}H-NMR (200 MHz, $CDCl_3$) δ: 1.29 (3H, t, J=7), 1.66 (3H, d, J=8), 4.12 (3H, s), 4.26 (1H, q, J=7), 6.60 (1H, dd, J=2, J=4), 6.74 (1H, bs), 7.31 (1H, d, J=4), 7.65 (1H, d, J=2), 8.20 (1H, s). HRMS m/z: $[M+Na]^+$ Calcd for $C_{16}H_{17}N_7O_3$ 378.1285, Found 378.1283 (Δ=0.0002).

2-((2-(Furan-2-yl)-8-methyl-8H-pyrazolo[4,3-e][1,2,4]triazolo[1,5-c]pyrimidin-5-yl)amino)-3-methylbutanoic acid ethyl ester (**2**): yield 28%; white solid; mp 152°C ^{1}H-NMR (200 MHz, $CDCl_3$) δ: 8.10 (1H, s), 7.64 (1H, s), 7.23 (1H, s), 6.72 (1H, d, *J*=9), 6.60 (1H, m), 5.00 (1H, dd, *J*=7, *J*=9), 4.26 (2H, q, *J*=7), 4.11 (3H, s), 2.52-2.36 (1H, m), 1.31 (3H, t, *J*=7), 1.09 (6H, d, *J*=7). HRMS m/z: $[M+Na]^+$ Calcd for $C_{18}H_{21}N_7O_3$ 406.1598, Found 406.1599 (Δ=0.0001).

2-(2-Furan-2-yl-8-methyl-8H-pyrazolo[4,3-e][1,2,4]triazolo[1,5-c]pyrimidin-5-ylamino)-4-methyl-pentanoic acid ethyl ester (**3**): yield 41%; pale orange solid; mp 145°C ^{1}H-NMR (200 MHz, $CDCl_3$) δ: 8.11 (1H, s), 7.64 (1H, d, *J*=2), 7.23 (1H, d, *J*=4), 6.60 (1H, dd, *J*=2, *J*=4), 6.29 (1H, d, *J*=8.8), 5.07 (1H, t, *J*=7), 4.22 (2H, q, *J*=7), 4.11 (3H, s), 1.86 (3H, m), 1.29 (3H, t, *J*=7), 1.01 (6H, d, *J*=5). HRMS m/z: $[M+Na]^+$ Calcd for $C_{19}H_{23}N_7O_3$ 420.1755, Found 420.1754 (Δ=0.0001).

2-((2-(Furan-2-yl)-8-methyl-8H-pyrazolo[4,3-e][1,2,4]triazolo[1,5-c]pyrimidin-5-yl)amino)hexanoic acid ethyl ester (**4**): yield 35%; orange solid; mp 75°C ^{1}H-NMR (200 MHz, $CDCl_3$) δ: 8.30 (1H, s), 7.66 (1H, s), 7.37 (1H, d, *J*=3.4), 6.75 (1H, d, *J*=8), 6.61 (1H, m), 5.08-4.95 (1H, m), 4.25 (2H, q, *J*=7), 4.12 (3H, s), 2.20-1.80 (2H, m), 1.41-1.27 (7H, m), 0.90 (3H, t, *J*=7). HRMS m/z: $[M+Na]^+$ Calcd for $C_{19}H_{23}N_7O_3$ 420.1755, Found 420.1757 (Δ=0.0002).

2-((2-(Furan-2-yl)-8-methyl-8H-pyrazolo[4,3-e][1,2,4]triazolo[1,5-c]pyrimidin-5-yl)amino)-2-phenylacetic acid ethyl ester (**5**): yield 34%; white solid; mp 189°C ^{1}H-NMR (200 MHz, $CDCl_3$) δ: 8.08 (1H, s), 7.62-7.54 (3H, m), 7.39-7.36 (3H, m), 7.22-7.14 (2H, m), 6.59 (1H, d, *J*=1.6), 5.99 (1H, d, *J*=7.4), 4.29-4.10 (5H, m), 1.25 (3H, t, *J*=7.2). HRMS m/z: $[M+H]^+$ Calcd for $C_{21}H_{19}N_7O_3$ 418.1622, Found 418.1620 (Δ=0.0002).

(R)-2-((2-(Furan-2-yl)-8-methyl-8H-pyrazolo[4,3-e][1,2,4]triazolo[1,5-c]pyrimidin-5-yl)amino)-3-(1H-indol-2-yl)propanoic acid ethyl ester (**6**): yield 42%; pale yellow solid; mp 128°C ^{1}H-NMR (200 MHz, $CDCl_3$) δ: 8.23 (1H, s), 8.10 (1H, s), 7.60 (2H, bs), 7.35-7.08 (6H, m), 6.79 (1H, d, *J*=12), 5.40-5.21 (1H, m), 4.17-4.10 (5H, m), 3.56 (2H, m), 1.20 (3H, t, *J*=7.1). HRMS m/z: $[M+H]^+$ Calcd for $C_{24}H_{22}N_8O_3$ 471.1888, Found 471.1889 (Δ=0.0001).

2-((2-(Furan-2-yl)-8-methyl-8H-pyrazolo[4,3-e][1,2,4]triazolo[1,5-c]pyrimidin-5-yl)amino)-3-hydroxypropanoic acid ethyl ester (**7**): yield 39%; white solid; mp 188°C ^{1}H-NMR (200 MHz, $CDCl_3$) δ: 7.69 (1H, s), 7.65 (1H, s), 7.23 (1H, d, *J*=3.8), 7.06 (1H, d, *J*=8), 6.61 (1H, dd, *J*=1.6, *J*=4), 5.05-4.98 (1H, m), 4.48-4.19 (4H, m), 4.05 (3H, s), 1.35 (3H, t, *J*=7.2). HRMS m/z: $[M+Na]^+$ Calcd for $C_{16}H_{17}N_7O_4$ 394.1234, Found 394.1230 (Δ=0.0004).

(S)-2-((2-(Furan-2-yl)-8-methyl-8H-pyrazolo[4,3-e][1,2,4]triazolo[1,5-c]pyrimidin-5-yl)amino)-3-(4-hydroxyphenyl)propanoic acid ethyl ester (**8**): yield 23%; brown sticky foam ^{1}H-NMR (200 MHz, $CDCl_3$) δ: 8.06 (1H, s), 7.60-7.59 (1H, m), 7.18-7.16 (1H, m), 7.08 (2H, d, *J*=8.4), 6.84 (2H, d, *J*=8.4), 6.72 (1H, d, *J*=8.0), 6.55 (1H, dd, *J*=1.8, *J*=3.2), 5.24-5.14 (1H, m), 4.19 (2H, q, *J*=7.2), 4.09 (s, 3H), 3.52 (1H, dd, *J*=8.0, *J*=16.0), 3.22 (1H, dd, *J*=8.0, *J*=16.0), 1.23 (3H, t, *J*=7.2). H of hydroxy group not detected. HRMS m/z: $[M+H]^+$ Calcd for $C_{22}H_{21}N_7O_4$ 448.1728, Found 448.1724 (Δ=0.0004).

(S)-2-((2-(Furan-2-yl)-8-methyl-8H-pyrazolo[4,3-e][1,2,4]triazolo[1,5-c]pyrimidin-5-yl)amino)-3-phenylpropanoic acid ethyl ester (**9**): yield 36%; brown sticky foam ^{1}H-NMR (200 MHz, $CDCl_3$) δ: 8.15 (1H, s), 7.63 (1H, s), 7.30-7.24 (6H, m), 6.72 (1H, d, *J*=8.2), 6.59 (1H, bs), 5.32-5.24 (1H, m), 4.25-4.12 (5H, m), 3.41-3.33 (2H, m), 1.24 (3H, t, *J*=7.2). HRMS m/z: $[M+H]^+$ Calcd for $C_{22}H_{21}N_7O_3$ 432.1779, Found 432.1778 (Δ=0.0001).

2-((2-(Furan-2-yl)-8-methyl-8H-pyrazolo[4,3-e][1,2,4]triazolo[1,5-c]pyrimidin-5-yl)amino)-3-hydroxy-3-phenylpropanoic acid ethyl ester (**10**): yield 31%; white solid; mp 195°C ^{1}H-NMR (200 MHz, $CDCl_3$) δ: 8.04 (1H, s), 7.63 (1H, s), 7.50-7.47 (2H, m), 7.33-7.21 (4H, m), 7.01 (1H, d, *J*=9.2), 6.58 (1H, bs), 5.49 (1H, bs), 5.30 (1H, dd, *J*=3.4, *J*=9.2), 4.21 (2H, q, *J*=7.0), 4.07 (3H, s), 3.04 (1H, bs), 1.22 (3H, t, *J*=7.0). HRMS m/z: $[M+H]^+$ Calcd for $C_{22}H_{21}N_7O_4$ 448.1728, Found 448.1726 (Δ=0.0002).

(S)-2-((2-(Furan-2-yl)-8-methyl-8H-pyrazolo[4,3-e][1,2,4]triazolo[1,5-c]pyrimidin-5-yl)amino)succinic acid diethyl ester (**11**): yield 44%; brown sticky foam ^{1}H-NMR (200 MHz, $CDCl_3$) δ: 8.09 (1H, s), 7.52 (1H, s), 7.21-7.14 (2H, m), 6.59 (1H, bs), 5.29-5.25 (1H, m), 4.29-4.11 (7H, m), 3.19-3.17 (2H, m), 1.32-1.23 (6H, m). HRMS m/z: $[M+H]^+$ Calcd for $C_{19}H_{21}N_7O_5$ 428.1677, Found 428.1679 (Δ=0.0002); $[M+Na]^+$ Calcd for $C_{19}H_{21}N_7O_5$ 450.1496, Found 450.1498 (Δ=0.0002).

(S)-2-((2-(Furan-2-yl)-8-methyl-8H-pyrazolo[4,3-e][1,2,4]triazolo[1,5-c]pyrimidin-5-yl)amino)pentanedioic acid diethyl ester (**12**): yield 37%; brown sticky foam ^{1}H-NMR (200 MHz, $CDCl_3$) δ: 8.09 (1H, s), 7.62 (1H, s), 7.22 (1H, d, *J*=4.4), 6.78 (1H, d, *J*=8.0), 6.59-5.58 (1H, m), 5.10-5.02 (1H, m), 4.31-4.07 (7H, m), 2.53-2.17 (4H, m), 1.41-1.18 (6H, m). HRMS m/z: $[M+H]^+$ Calcd for $C_{20}H_{23}N_7O_5$ 442.1833, Found 442.1832 (Δ=0.0001).

(S)-1-(2-(Furan-2-yl)-8-methyl-8H-pyrazolo[4,3-e][1,2,4]triazolo[1,5-c]pyrimidin-5-yl)pyrrolidine-2-carboxylic acid methyl ester (**13**): yield 43%; pale yellow solid; mp 104°C ^{1}H-NMR (200 MHz, $CDCl_3$) δ: 8.06 (1H, s), 7.60-7.59 (1H, m), 7.13-7.11 (1H, m), 6.56-6.55 (1H, m), 5.48-5.36 (1H, m), 4.28-4.09 (5H, m), 3.74 (3H, s), 2.24-2.00 (4H, m). HRMS m/z: $[M+H]^+$ Calcd for $C_{17}H_{17}N_7O_3$ 368.1466, Found 368.1466 (Δ=0.0000).

4-(2-Furan-2-yl-8-methyl-8H-pyrazolo[4,3-e][1,2,4]triazolo[1,5-c]pyrimidin-5-ylamino)-butyric acid ethyl ester (**14**): yield 57%; pale yellow solid; mp 174°C ^{1}H-NMR (200 MHz, $CDCl_3$) δ: 1.25 (3H, t, J=7), 2.11 (2H, quint, J=7), 2.47 (2H, t, J=7), 3.51 (2H, q, J=7), 4.11-4.20 (5H, m), 6.38 (1H, bs), 6.59 (1H, dd, J=2, J=4), 7.20 (1H, d, J=4), 7.62 (1H, d, J=2), 8.09 (1H, s). HRMS m/z: $[M+Na]^+$ Calcd for $C_{17}H_{19}N_7O_3$ 392.1442, Found 392.1443 (Δ=0.0001).

Biology

Radioligand binding to hA_1, hA_{2A} and hA_3 ARs. All performed binding studies have been performed as previously reported.[2] CHO cells transfected with human AR subtypes have been used to obtain membranes for radioligand binding. Removal of cell fragments and nuclei have been performed by centrifugation at low-speed (1,000 x g), then centrifugation at 100,000 x g led to the sedimentation of the crude membrane fraction. The membranes were resuspended in the appropriate buffer (50 mMTris/HCl buffer pH 7.4 for hA_1 and hA_{2A} AR; 50 mMTris/HCl,10 mM $MgCl_2$, 1 mM EDTA, pH 8.25 for hA_3 AR) and stored at -80 °C. 1 nM [^{3}H]CCPA, 10 nM [^{3}H]NECA and 1 nM [^{3}H]HEMADO were used as radioligands for hA_1, hA_{2A} and hA_3 ARs, respectively. [^{3}H]CCPA non specific binding was determined using theophylline (1 mM), while 100 μM R-PIA has been used for [^{3}H]NECA and [^{3}H]HEMADO.[2,3,4] SCTFIT was the program used for Ki values calculations that was the mean of 3-6 replicates.[5]

Adenylyl cyclase activity. Functional studies for the hA_{2B} AR were performed using adenylyl cyclase experiments. Minor modifications were carried out on the previously reported procedures.[2,6] In this experimental procedure the homogenate of hA_2B-CHO cells was subjected to high speed centrifugation and the sedimented membrane pellet was then resuspended in buffer (50 mMTris/HCl, pH 7.4) and directly used for the assay. Affinity of compounds was determined by inhibition of NECA-stimulated adenylyl cyclase activity (NECA, 5 μM). About 150,000 cpm of [α-^{32}P]ATP was incubated with membranes and the incubation mixture for 20 min without EGTA and NaCl.[6] Hill equation was used to calculate IC_{50} that was the mean of 3-6 replicates. Hill coefficients were near unity.

Computational studies

Molecular modeling operations were done with the MOE program[7] on a 12 CPU (Intel® Xeon® CPU E5-1650 3.80 GHz) Linux workstation. MD simulations were carried out using the ACEMD engine[8] and the CHARMM36/CHARMM36 general force field (CGenFF) on NVIDIA GTX 980Ti and NVIDIA GTX 980 drivers. The GOLD[9] software and the goldscore scoring function were used for docking simulations. Ligand structures were built with the MOE-builder tool. Ionization states were assigned by the MOE-protonate 3D implementation. Tautomers and hybridization were checked. The MMFF94x was used for the geometry optimizations (root mean square (RMS) gradient < 0.05 kcal mol^{-1} A^{-1}). The docking search space was assigned to a sphere of 20 Å radius, centered on the $N^{6.55}$ peptidic nitrogen. 20 poses were obtained for any ligand docked at each receptor subtype. Partial charges were assigned to the ligands and protein as provided by the MMFF94 and AMBER14:EHT[10] force fields, respectively. The hA_2 AR and the hA_1 ARs' atom positions were extracted from the Protein Data Bank[11] crystal structures 3PWH[12] and 5UEN[13], respectively. A homology model of the hA_3AR was adopted, constructed in our previous study (SI4).[14] Both molecular docking and MD simulations on ARs included the presence of the sodium ion and its first solvation shell.[15] In most cases, conserved residues were reported with the Ballesteros–Weinstein numbering.[16] Electrostatic, van der Waals and hydrophobic contributions reported in the IE fingerprints and in the per-residue histograms were calculated with MOE. Plots were drawn with Gnuplot 4.6.[17] Figures showing three-dimensional molecules were created using UCSF Chimera,[18] except Figure 8, for which the VMD-1.9.3 graphical interface was exploited.[19] Ligand parameters to use in MD simulations were obtained from the Paramchem web service. The 1-palmitoyl-2oleyl-sn-glycerol-

3-phospho-choline (POPC) lipid bilayer was generated as a model of the cell membrane. For this purpose the Orientations Proteins in Membrane (OPM) database coordinates[20] and the VMD membrane builder plugin were used. Lipid molecules within 0.4 Å of the protein were deleted and TIP3P[21] water molecules were included for solvation with Solvate1.0.[22] Na^+/Cl^- neutralizing counterions were added reaching a concentration of 0.154 M. System was equilibrated in three steps: 1) 1500 conjugate-gradient minimization steps to reduce lipid-protein steric clashes and a NPT ensemble MD simulation of 5 ns constraining the ligand, protein, and lipid phosphorus atom position at 1 kcal mol^{-1} $Å^{-2}$; 2) NPT MD simulation of 10 ns constraining the protein, the ligand, the sodium ion and its first solvation shell; 3) the coordinates of ligand, protein alpha carbons and sodium complex were constrained for 5 ns. A time step of 2 fs was used in any simulation along with the Berendsen barostat (1 atm),[23] the Langevin thermostat (temperature, 310 K; low dumping, 1 ps^{-1}),[24] the M-SHAKE algorithm [25] and a cutoff of 10 Å for long-range interactions. Ligand-protein interaction energy was calculated by means of the NAMD energy Plugin 1.4.[26]

References

1 S. Federico, A. Ciancetta, D. Sabbadin, S. Paoletta, G. Pastorin, B. Cacciari, K. N. Klotz, S. Moro and G. Spalluto, *J. Med. Chem.*, 2012, **55**, 9654–9668.

2 K.-N. Klotz, J. Hessling, J. Hegler, C. Owman, B. Kull, B. B. Fredholm and M. J. Lohse, *Naunyn. Schmiedebergs. Arch. Pharmacol.*, 1998, **357**, 1–9.

3 K.-N. Klotz, E. Camaioni, R. Volpini, S. Kachler, S. Vittori and G. Cristalli, *Naunyn. Schmiedebergs. Arch. Pharmacol.*, 1999, **360**, 103–108.

4 K. N. Klotz, N. Falgner, S. Kachler, C. Lambertucci, S. Vittori, R. Volpini and G. Cristalli, *Eur. J. Pharmacol.*, 2007, **556**, 14–18.

5 A. De Lean, A. A. Hancock and R. J. Lefkowitz, *Mol. Pharmacol.*, 1982, **21**, 5–16.

6 K. N. Klotz, G. Cristalli and M. Grifantini, *J. Biol. Chem.*, 1985, **260**, 14659–14664.

7 Chemical Computing Group (CCG) Inc., 2016.

8 A. D. MacKerell, N. Banavali and N. Foloppe, *Biopolymers*, 2000, **56**, 257–265.

9 The Cambridge Crystallographic Data Centre (CCDC), .

10 J. Wang, R. M. Wolf, J. W. Caldwell, P. A. Kollman and D. A. Case, *J. Comput. Chem.*, 2004, **25**, 1157–1174.

11 H. M. Berman, J. Westbrook, Z. Feng, G. Gilliland, T. N. Bhat, H. Weissig, I. N. Shindyalov and P. E. Bourne, *Nucleic Acids Res.*, 2000, **28**, 235–242.

12 A. S. Doré, N. Robertson, J. C. Errey, I. Ng, K. Hollenstein, B. Tehan, E. Hurrell, K. Bennett, M. Congreve, F. Magnani, C. G. Tate, M. Weir and F. H. Marshall, *Structure*, 2011, **19**, 1283–1293.

13 A. Glukhova, D. M. Thal, A. T. Nguyen, E. A. Vecchio, M. Jörg, P. J. Scammells, L. T. May, P. M. Sexton and A. Christopoulos, *Cell*, 2017, **168**, 867-877.e13.

14 E. Margiotta and S. Moro, *Appl. Sci.*, 2019, **9**, 821.

15 S. Federico, E. Margiotta, S. Paoletta, S. Kachler, K.-N. Klotz, K. A. Jacobson, G. Pastorin, S. Moro and G. Spalluto, *Medchemcomm*, 2019, **10**, 1094–1108.

16 J. A. Ballesteros and H. Weinstein, *Methods Neurosci.*, 1995, **25**, 366–428.

17 Gnuplot, (n.d.). http://www.gnuplot.info/download.html.

18 E. F. Pettersen, T. D. Goddard, C. C. Huang, G. S. Couch, D. M. Greenblatt, E. C. Meng and T. E. Ferrin, *J. Comput. Chem.*, 2004, **25**, 1605–1612.

19 W. Humphrey, A. Dalke and K. Schulten, *J Mol Graph*, 1996, **14**, 27, 33–38.

20 M. A. Lomize, A. L. Lomize, I. D. Pogozheva and H. I. Mosberg, *Bioinformatics*, 2006, **22**, 623–625.

21 W. L. Jorgensen, J. Chandrasekhar, J. D. Madura, R. W. Impey and M. L. Klein, *J. Chem. Phys.*, 1983, **79**, 926–935.

22 Grubmuller H. and Groll V., 1996. Solvate | Max Planck Institute for Biophysical Chemistry. https://www.mpibpc.mpg.de/grubmueller/solvate (accessed August 7, 2019).

23 H. J. C. Berendsen, J. P. M. Postma, W. F. van Gunsteren, A. DiNola and J. R. Haak, *J. Chem. Phys.*, 1984, **81**, 3684–3690.

24 R. J. Loncharich, B. R. Brooks and R. W. Pastor, *Biopolymers*, 1992, **32**, 523–535.

25 U. Essmann, L. Perera, M. L. Berkowitz, T. Darden, H. Lee and L. G. Pedersen, *J. Chem. Phys.*, 1995, **103**, 8577–8593.

26 J. C. Phillips, R. Braun, W. Wang, J. Gumbart, E. Tajkhorshid, E. Villa, C. Chipot, R. D. Skeel, L. Kalé and K. Schulten, *J. Comput. Chem.*, 2005, **26**, 1781–1802.

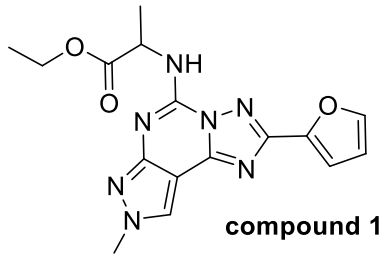
O
O
NH
N
N
N
O
N
N
N

compound 1

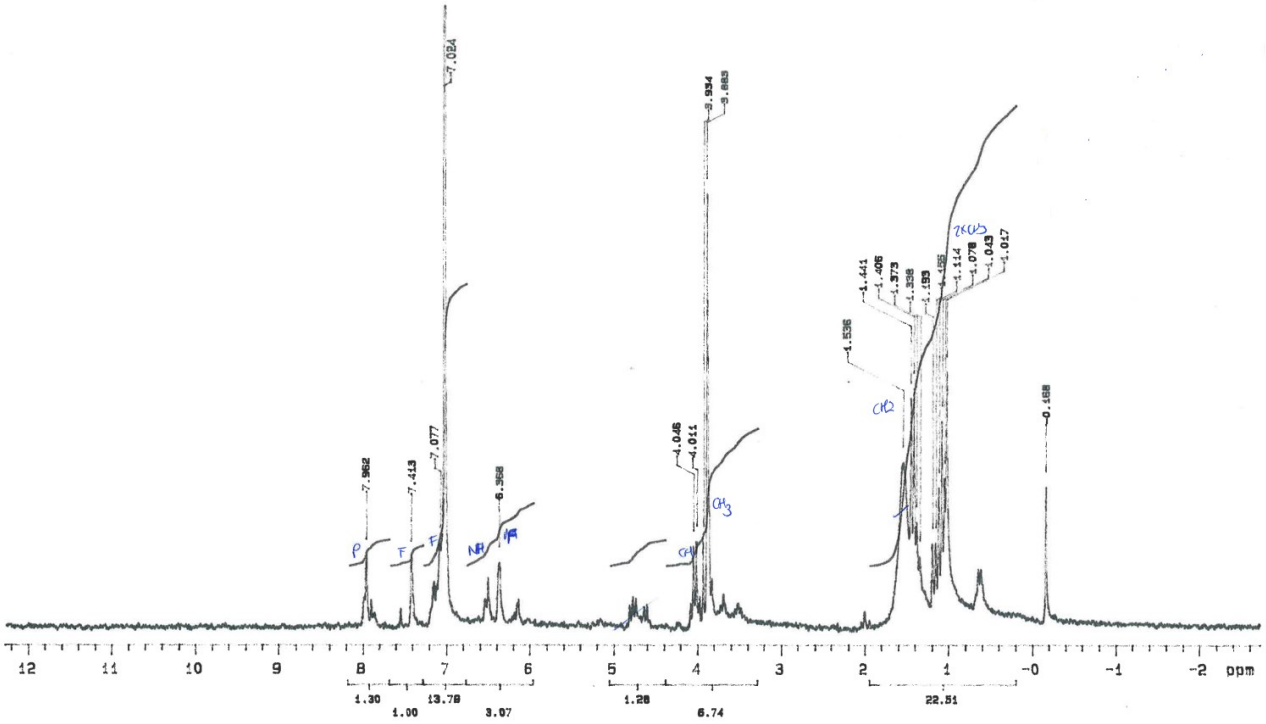
7.962
7.413
7.077
7.084
6.958
8.934
8.883
4.046
4.011
1.536
1.441
1.406
1.373
1.338
1.193
1.114
1.078
1.043
1.017
0.168
CH2
CH3
12
11
10
9
8
7
6
5
4
3
2
1
-0
-1
-2
ppm
1.30
1.00
13.78
3.07
1.28
6.74
22.51

Display Report

Analysis Info

Analysis Name	D:\Data\Prato\26.02.20\WS104.d	Acquisition Date	2/26/2020 10:31:23 AM
Method	Leu-Enk.m	Operator	BDAL@DE
Sample Name		Instrument	micrOTOF-Q 8228888.00052
Comment			

Acquisition Parameter

Source Type	ESI	Ion Polarity	Positive	Set Nebulizer	0.4 Bar
Focus	Not active	Set Capillary	4500 V	Set Dry Heater	200 °C
Scan Begin	50 m/z	Set End Plate Offset	-500 V	Set Dry Gas	4.0 l/min
Scan End	1000 m/z	Set Collision Cell RF	350.0 Vpp	Set Divert Valve	Source

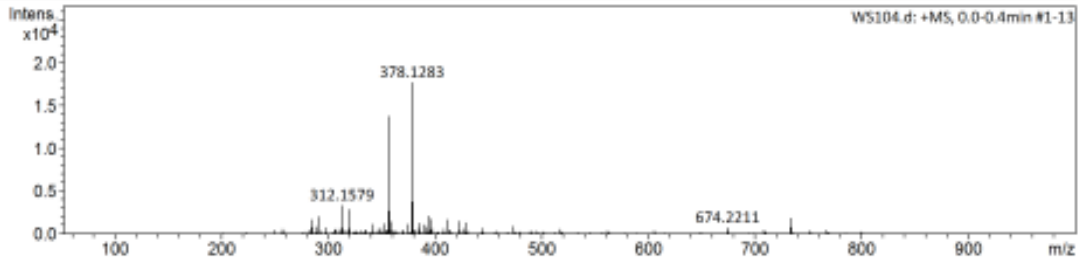

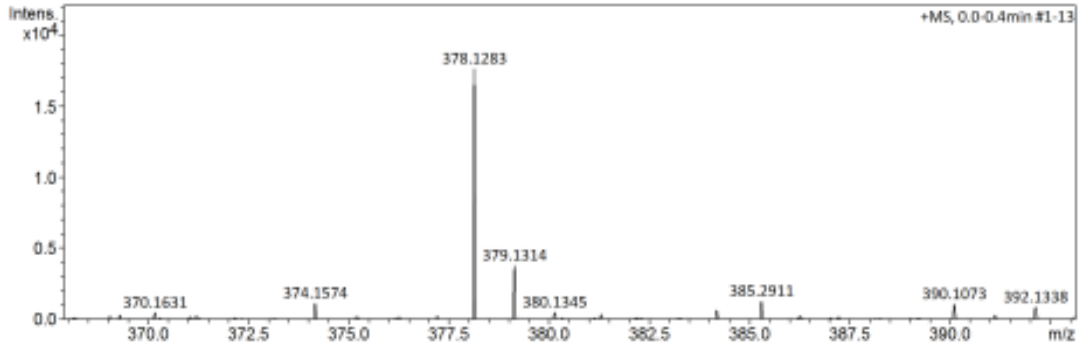

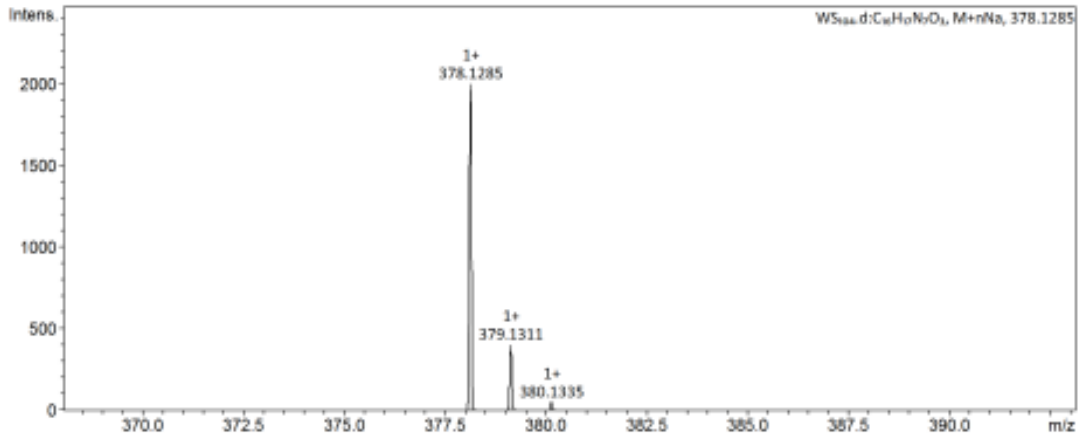

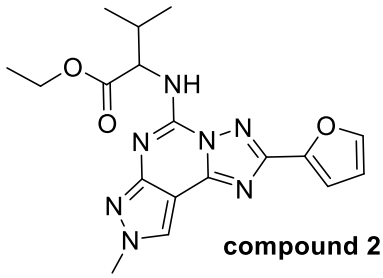
O
NH
O
N
N
N
N
N
O
N

compound 2

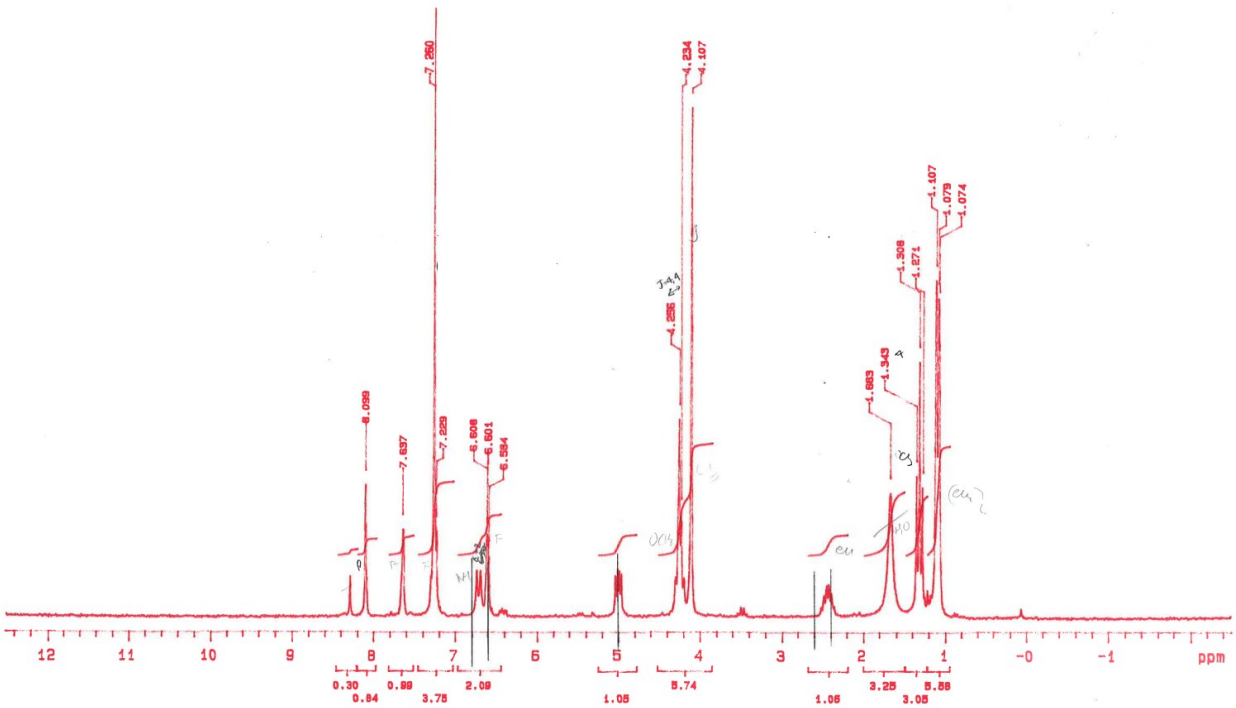
8.099
7.837
7.260
7.229
6.606
6.601
6.584
4.234
4.107
4.255
1.683
1.343
1.308
1.271
1.107
1.079
1.074
12
11
10
9
8
7
6
5
4
3
2
1
-0
-1
ppm
0.30
0.84
0.89
3.75
2.09
1.05
5.74
1.06
3.25
5.88
3.05

Display Report

Analysis Info

Analysis Name	D:\Data\Prato\26.02.20\WS137.d	Acquisition Date	2/26/2020 10:56:35 AM
Method	Leu-Enk.m	Operator	BDAL@DE
Sample Name		Instrument	micrOTOF-Q 8228888.00052
Comment			

Acquisition Parameter

Source Type	ESI	Ion Polarity	Positive	Set Nebulizer	0.4 Bar
Focus	Not active	Set Capillary	4500 V	Set Dry Heater	200 °C
Scan Begin	50 m/z	Set End Plate Offset	-500 V	Set Dry Gas	4.0 l/min
Scan End	1000 m/z	Set Collision Cell RF	350.0 Vpp	Set Divert Valve	Source

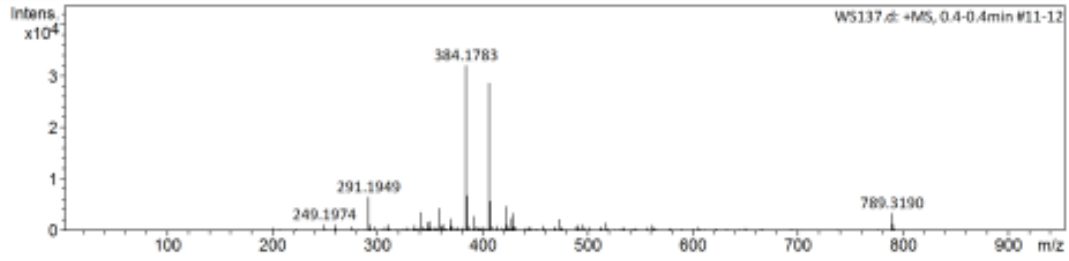

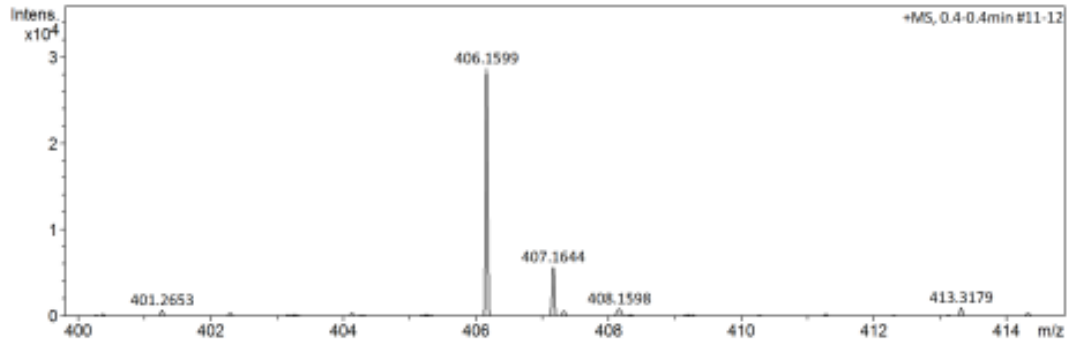

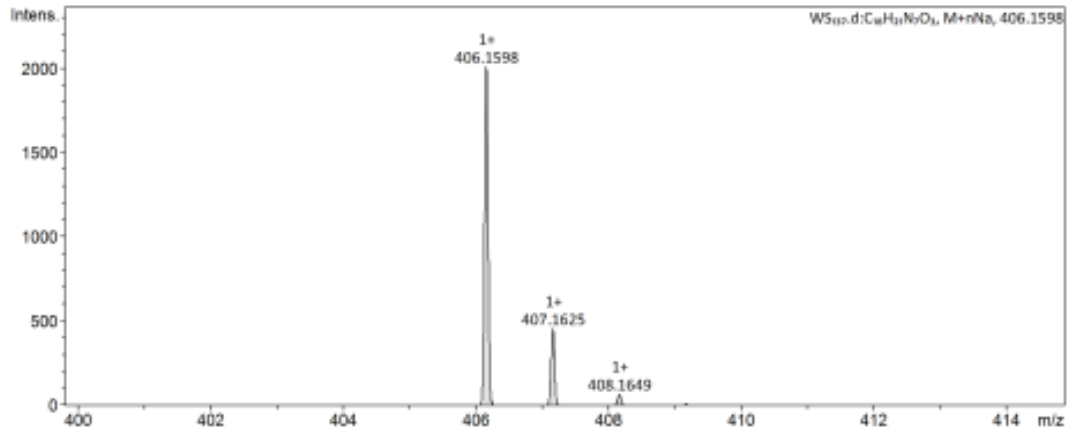

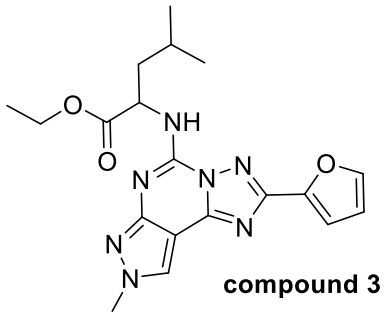
O
O
NH
N
N
N
N
N
O
N

compound 3

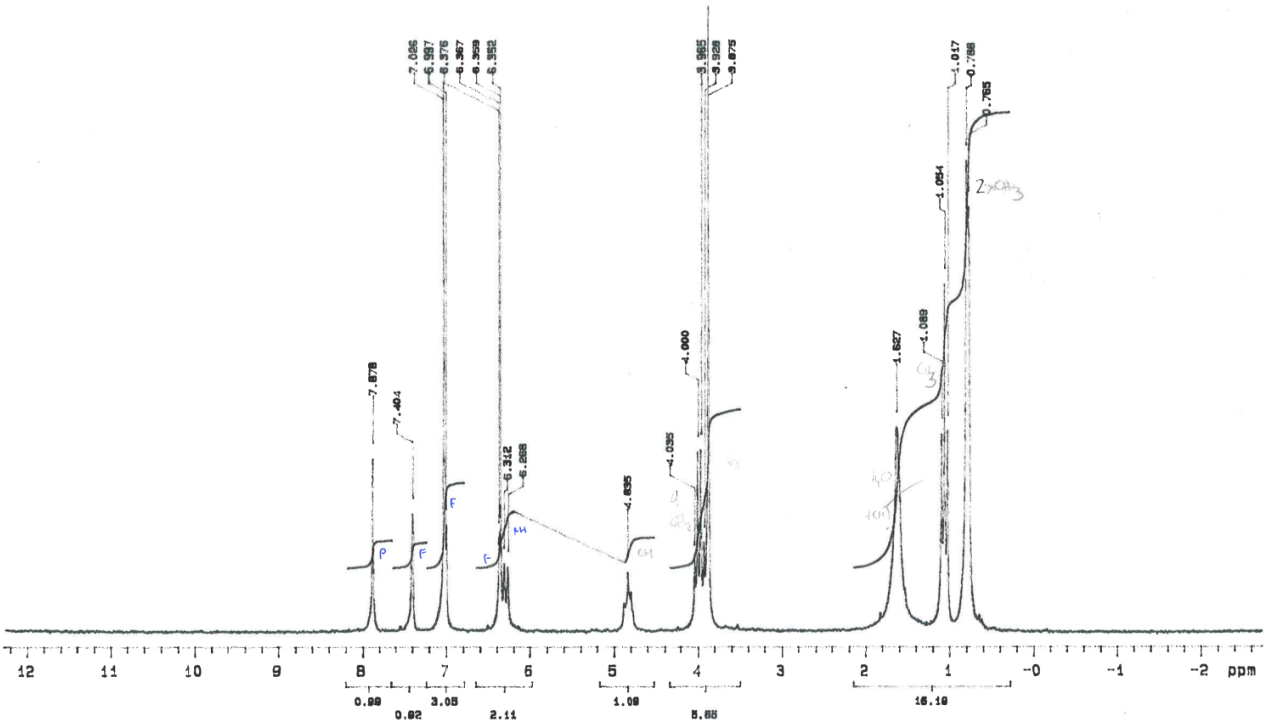
7.878
7.404
6.342
6.288
4.000
4.035
4.025
1.627
1.089
1.054
1.017
0.788
0.765
12
11
10
9
8
7
6
5
4
3
2
1
-0
-1
-2
ppm
0.99
0.82
3.05
2.11
1.09
5.88
16.10

Display Report

Analysis Info

Analysis Name	D:\Data\Prato\26.02.20\WS105.d	Acquisition Date	2/26/2020 10:39:47 AM
Method	Leu-Enk.m	Operator	BDAL@DE
Sample Name		Instrument	micrOTOF-Q 8228888.00052
Comment			

Acquisition Parameter

Source Type	ESI	Ion Polarity	Positive	Set Nebulizer	0.4 Bar
Focus	Not active	Set Capillary	4500 V	Set Dry Heater	200 °C
Scan Begin	50 m/z	Set End Plate Offset	-500 V	Set Dry Gas	4.0 l/min
Scan End	1000 m/z	Set Collision Cell RF	350.0 Vpp	Set Divert Valve	Source

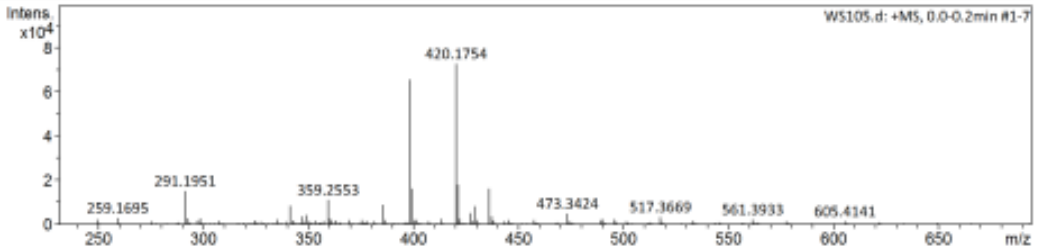

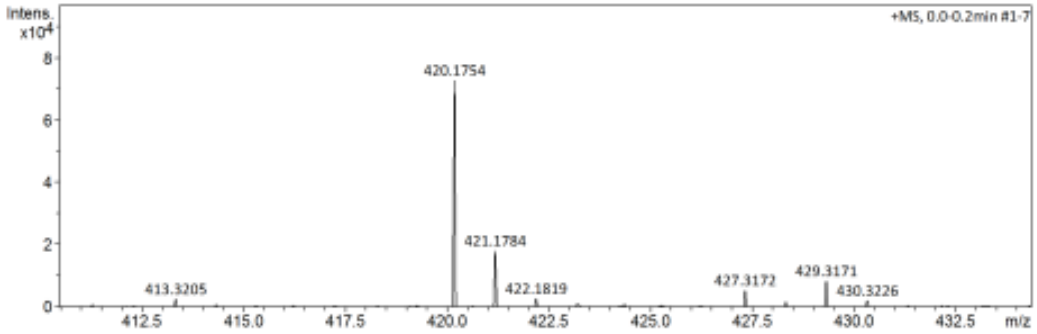

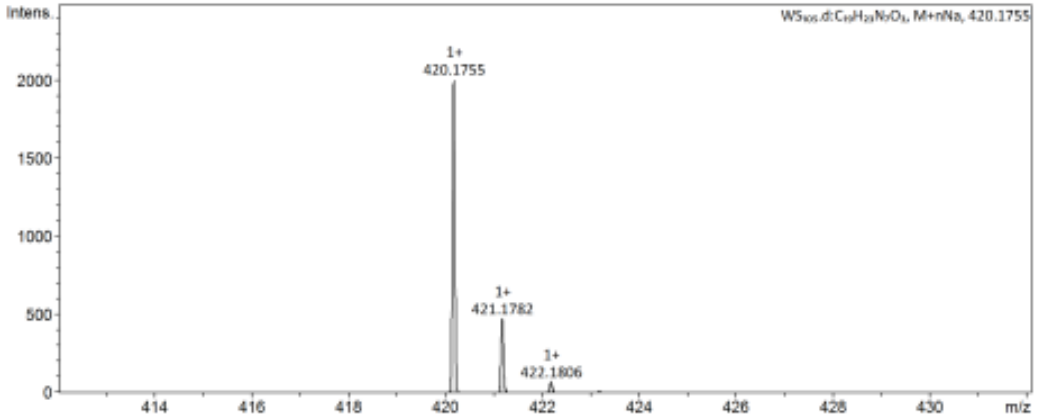

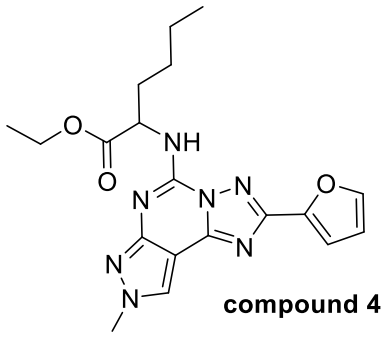
O
NH
O
N
N
N
N
N
O
N

compound 4

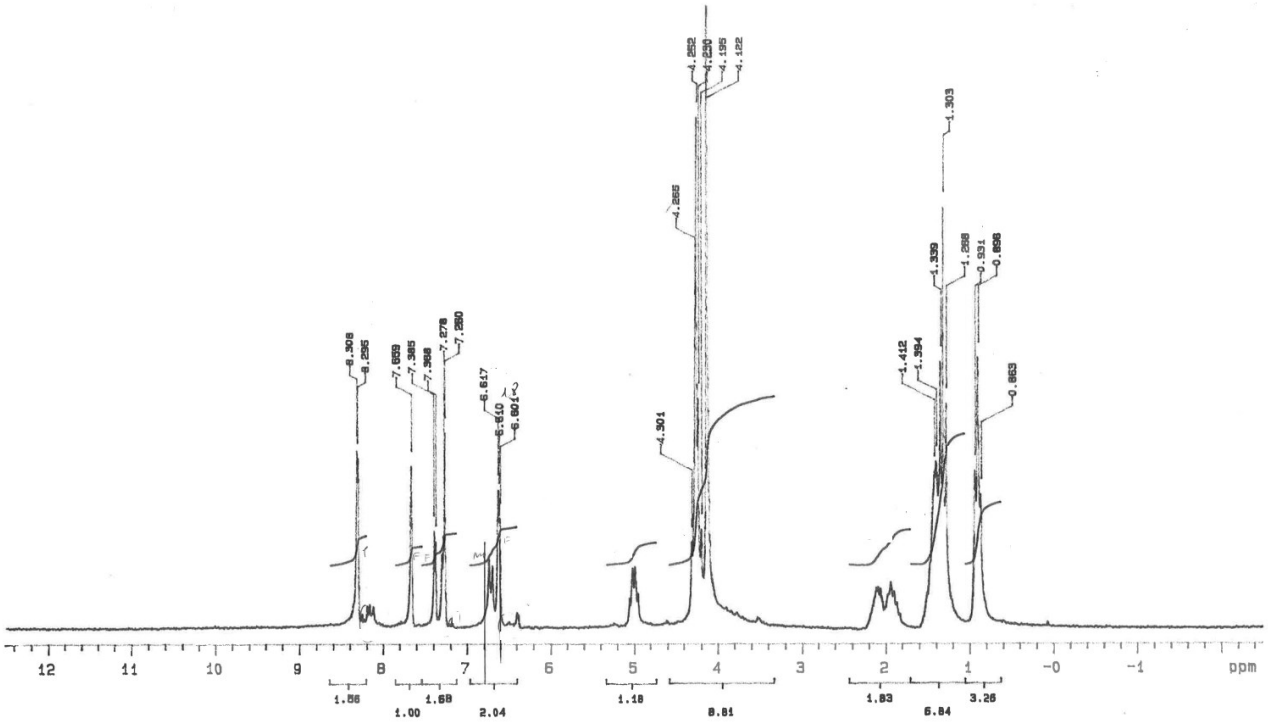
8.308
8.295
7.669
7.385
7.368
7.278
7.260
6.617
6.610
6.604
4.501
4.265
4.252
4.250
4.195
4.122
1.412
1.394
1.339
1.303
1.288
0.931
0.858
0.863
12
11
10
9
8
7
6
5
4
3
2
1
-0
-1
ppm
1.56
1.00
1.68
2.04
1.18
8.81
1.83
5.84
3.26

Display Report

Analysis Info

Analysis Name	D:\Data\Prato\26.02.20\WS138.d	Acquisition Date	2/26/2020 11:09:23 AM
Method	Leu-Enk.m	Operator	BDAL@DE
Sample Name		Instrument	micrOTOF-Q 8228888.00052
Comment			

Acquisition Parameter

Source Type	ESI	Ion Polarity	Positive	Set Nebulizer	0.4 Bar
Focus	Not active	Set Capillary	4500 V	Set Dry Heater	200 °C
Scan Begin	50 m/z	Set End Plate Offset	-500 V	Set Dry Gas	4.0 l/min
Scan End	1000 m/z	Set Collision Cell RF	350.0 Vpp	Set Divert Valve	Source

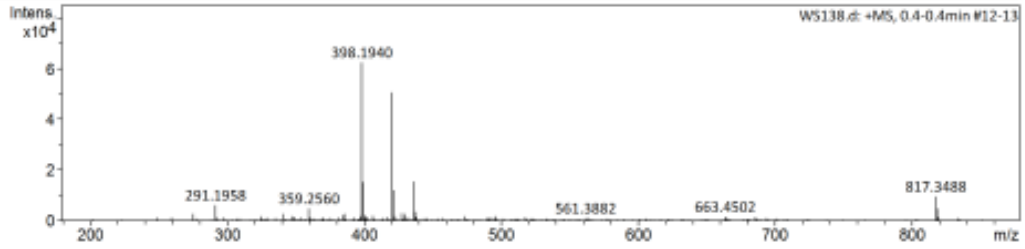

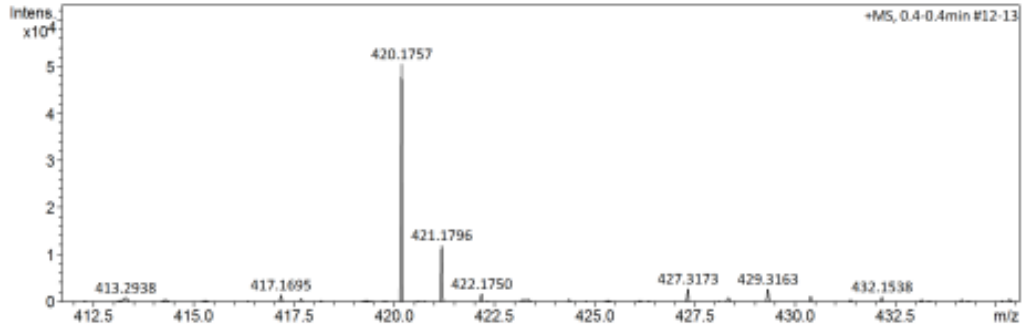

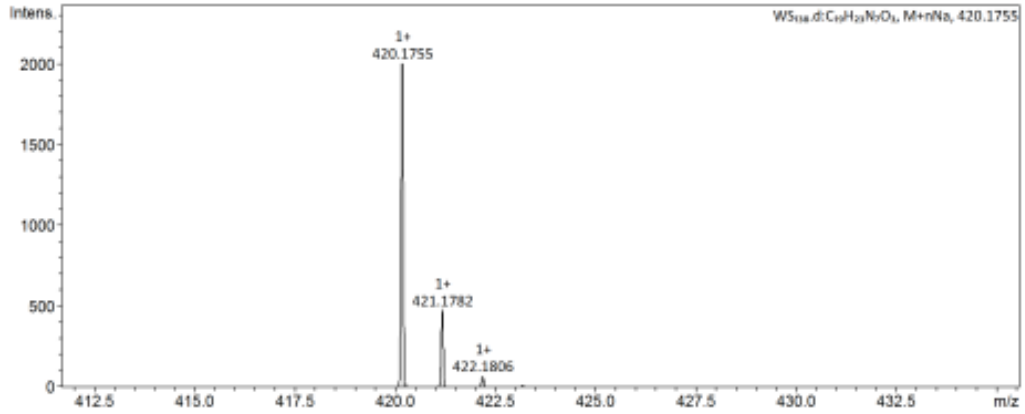

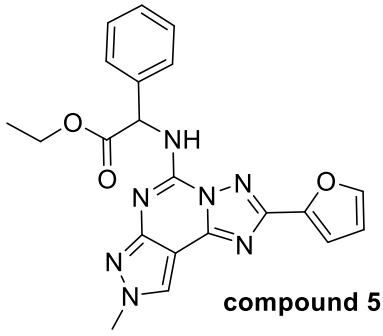
O
NH
O
N
N
N
N
N
O

compound 5

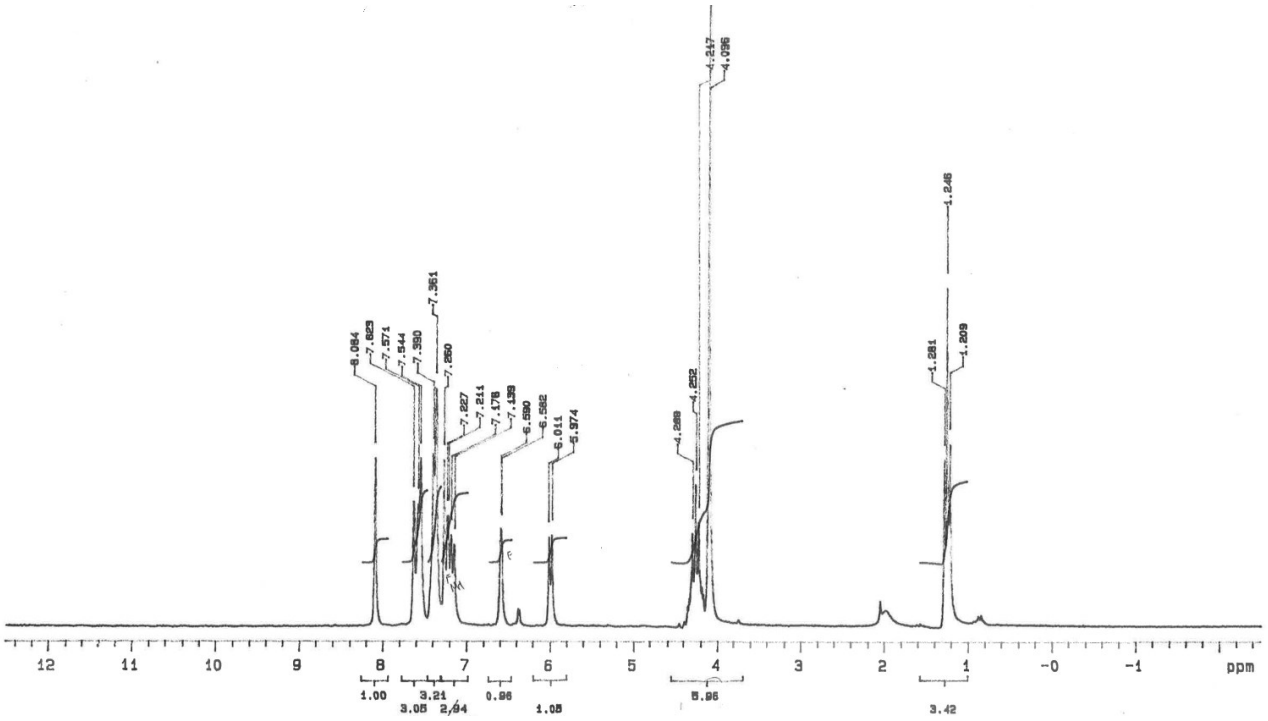
8.084
7.823
7.571
7.544
7.380
7.361
7.260
7.227
7.211
7.178
7.139
6.580
6.582
6.011
5.974
4.289
4.252
4.217
4.096
1.846
1.281
1.209
12
11
10
9
8
7
6
5
4
3
2
1
-0
-1
ppm
1.00
3.21
3.05
2.94
0.96
1.08
5.96
3.42

Display Report

Analysis Info

Analysis Name	D:\Data\Prato\26.02.20\WS139.d	Acquisition Date	2/26/2020 11:21:20 AM
Method	Leu-Enk.m	Operator	BDAL@DE
Sample Name		Instrument	micrOTOF-Q 8228888.00052
Comment			

Acquisition Parameter

Source Type	ESI	Ion Polarity	Positive	Set Nebulizer	0.4 Bar
Focus	Not active	Set Capillary	4500 V	Set Dry Heater	200 °C
Scan Begin	50 m/z	Set End Plate Offset	-500 V	Set Dry Gas	4.0 l/min
Scan End	1000 m/z	Set Collision Cell RF	350.0 Vpp	Set Divert Valve	Source

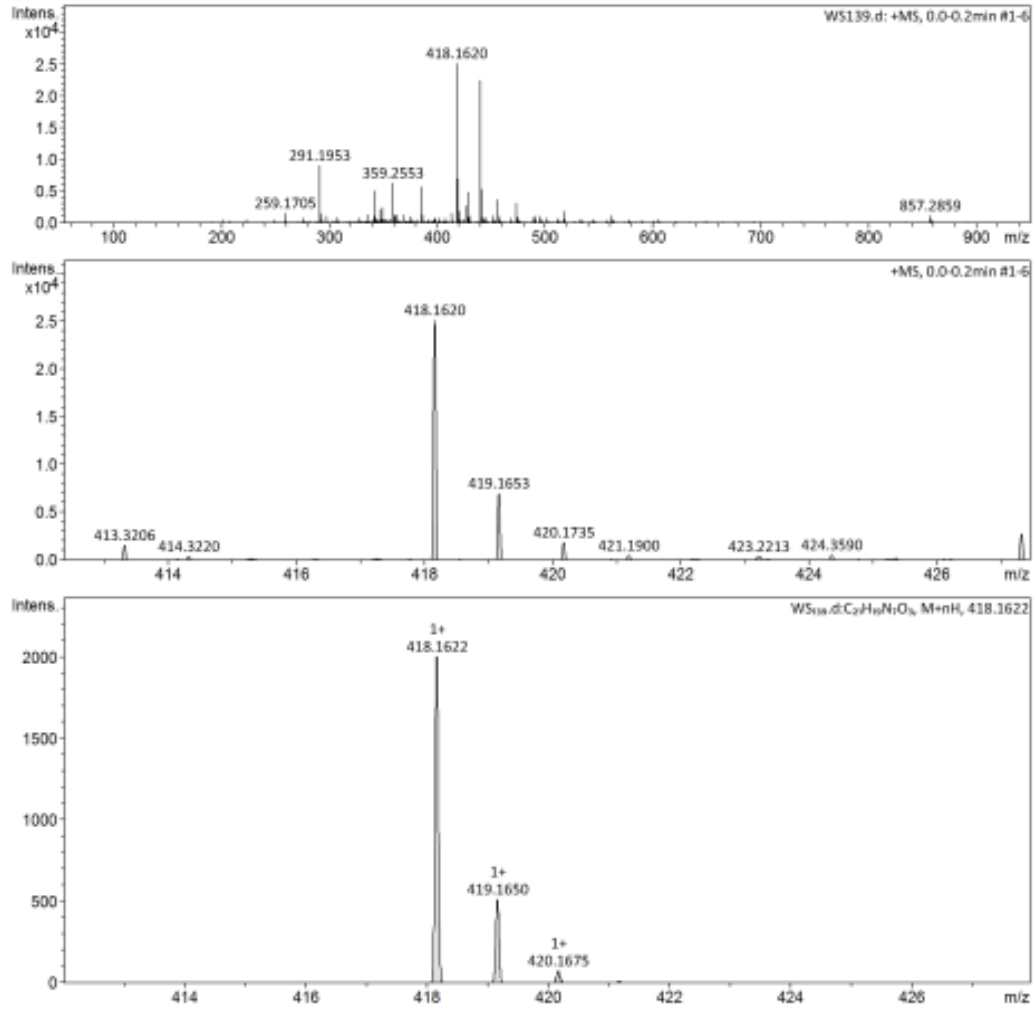

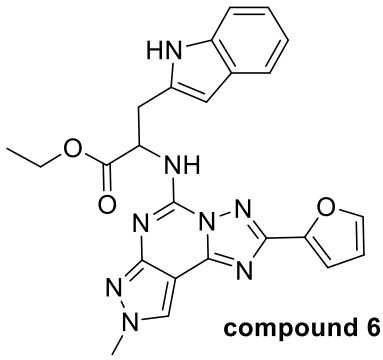
HN
O
NH
O
N
N
N
O
N
N
N

compound 6

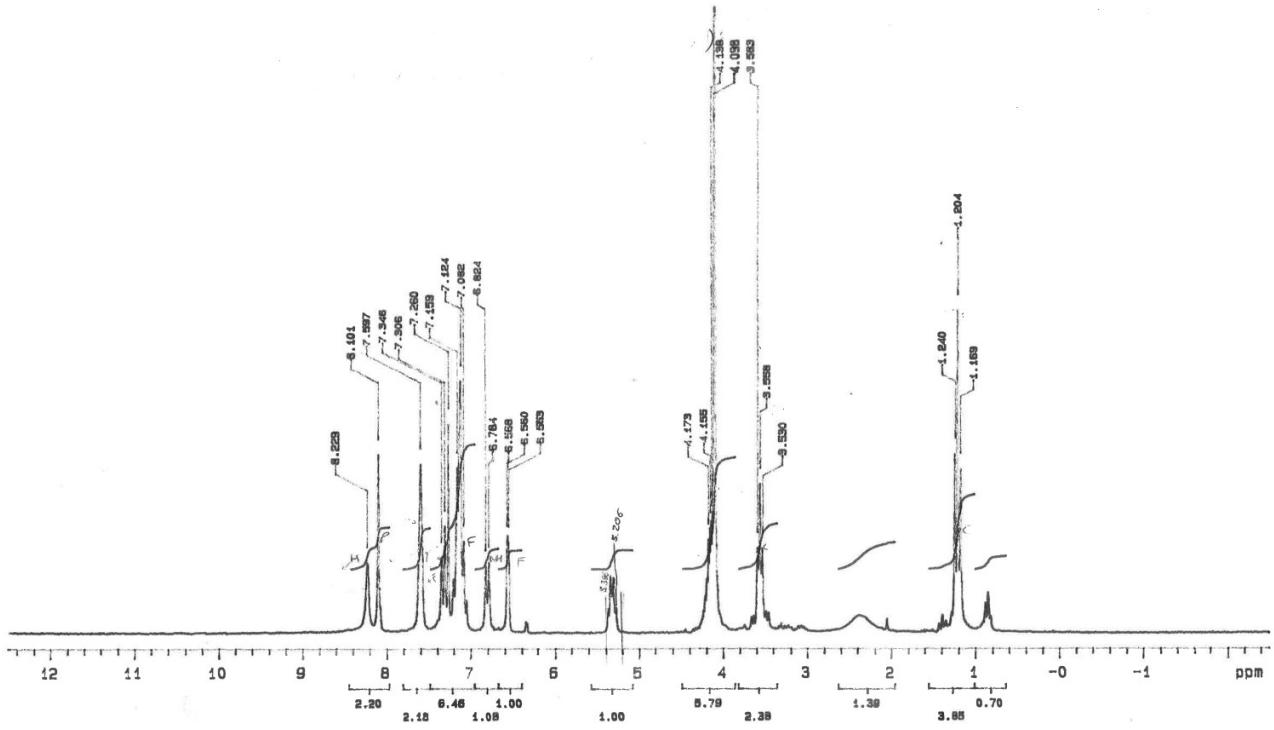
12
11
10
9
8
7
6
5
4
3
2
1
-0
-1
ppm
2.20
2.15
6.46
1.08
1.00
1.00
5.79
2.38
1.39
3.85
0.70

Display Report

Analysis Info

Analysis Name	D:\Data\Prato\26.02.20\WS140.d	Acquisition Date	2/26/2020 11:30:24 AM
Method	Leu-Enk.m	Operator	BDAL@DE
Sample Name		Instrument	micrOTOF-Q 8228888.00052
Comment			

Acquisition Parameter

Source Type	ESI	Ion Polarity	Positive	Set Nebulizer	0.4 Bar
Focus	Not active	Set Capillary	4500 V	Set Dry Heater	200 °C
Scan Begin	50 m/z	Set End Plate Offset	-500 V	Set Dry Gas	4.0 l/min
Scan End	1000 m/z	Set Collision Cell RF	350.0 Vpp	Set Divert Valve	Source

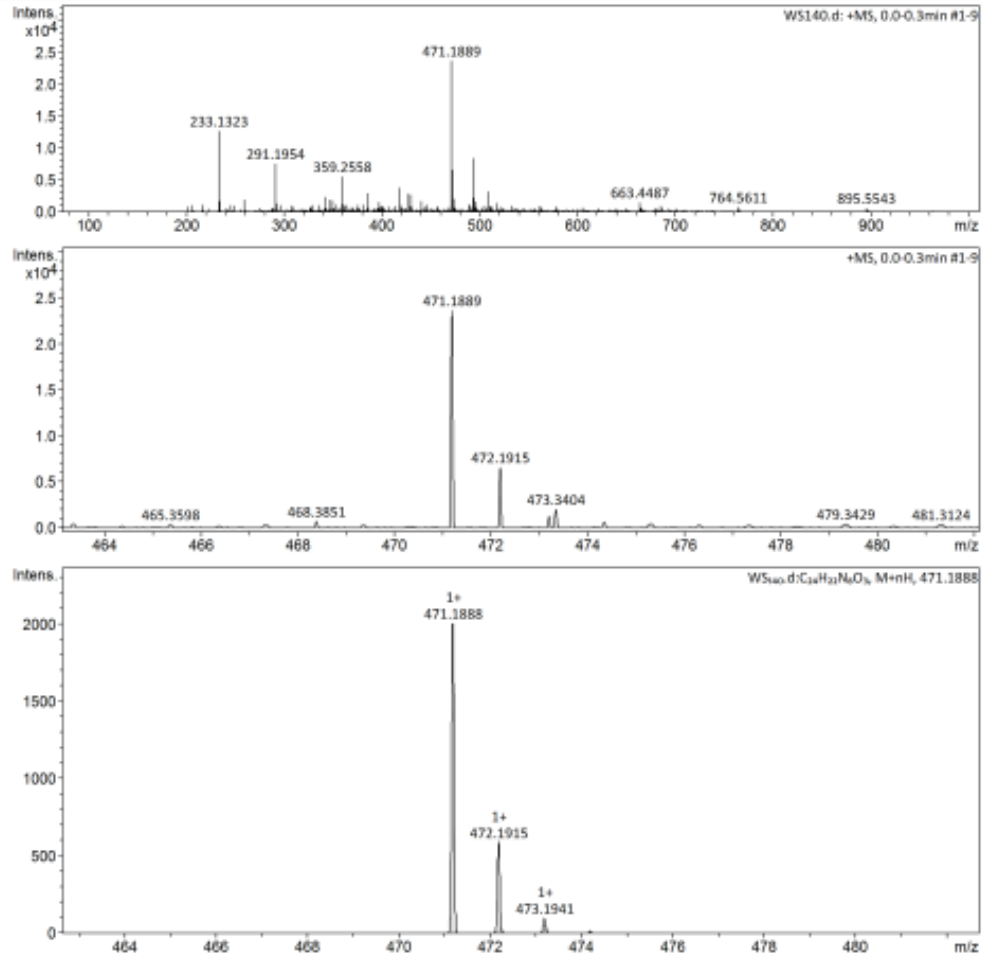

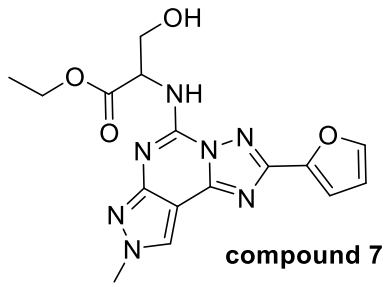
OH
O
NH
O
N
N
N
O
N
N
N

compound 7

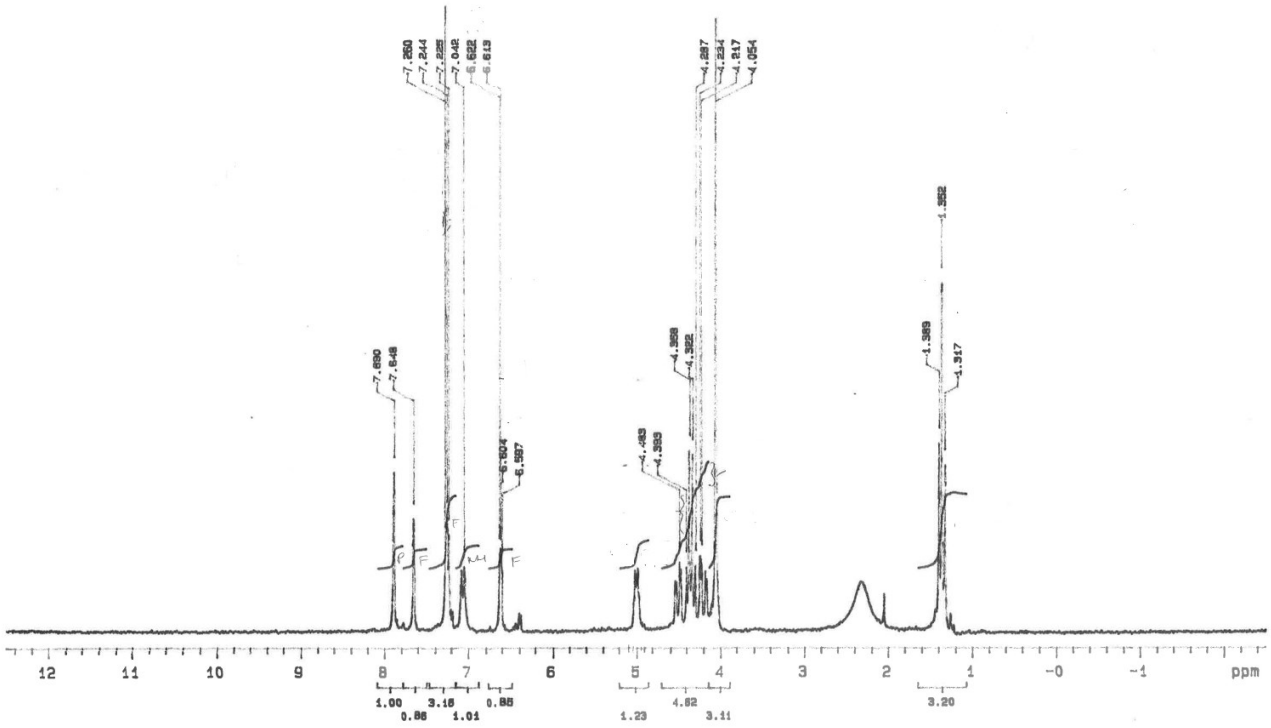
12
11
10
9
8
7
6
5
4
3
2
1
-0
-1
ppm
1.00
3.18
1.01
0.88
0.85
1.23
4.82
3.11
3.20

Display Report

Analysis Info

Analysis Name	D:\Data\Prato\26.02.20\WS141.d	Acquisition Date	2/26/2020 11:43:04 AM
Method	Leu-Enk.m	Operator	BDAL@DE
Sample Name		Instrument	micrOTOF-Q 8228888.00052
Comment			

Acquisition Parameter

Source Type	ESI	Ion Polarity	Positive	Set Nebulizer	0.4 Bar
Focus	Not active	Set Capillary	4500 V	Set Dry Heater	200 °C
Scan Begin	50 m/z	Set End Plate Offset	-500 V	Set Dry Gas	4.0 l/min
Scan End	1000 m/z	Set Collision Cell RF	350.0 Vpp	Set Divert Valve	Source

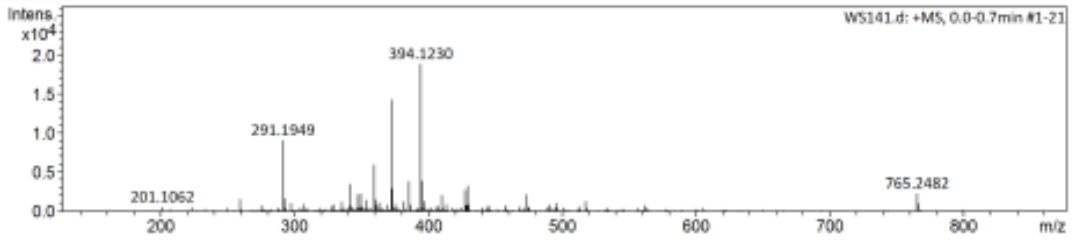

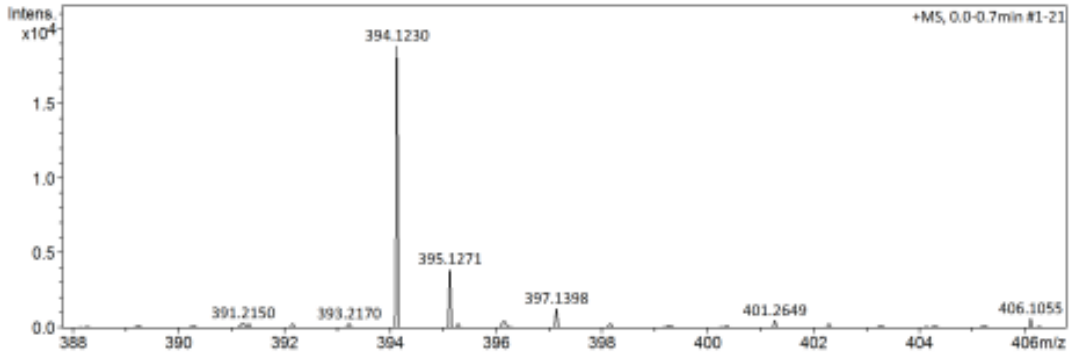

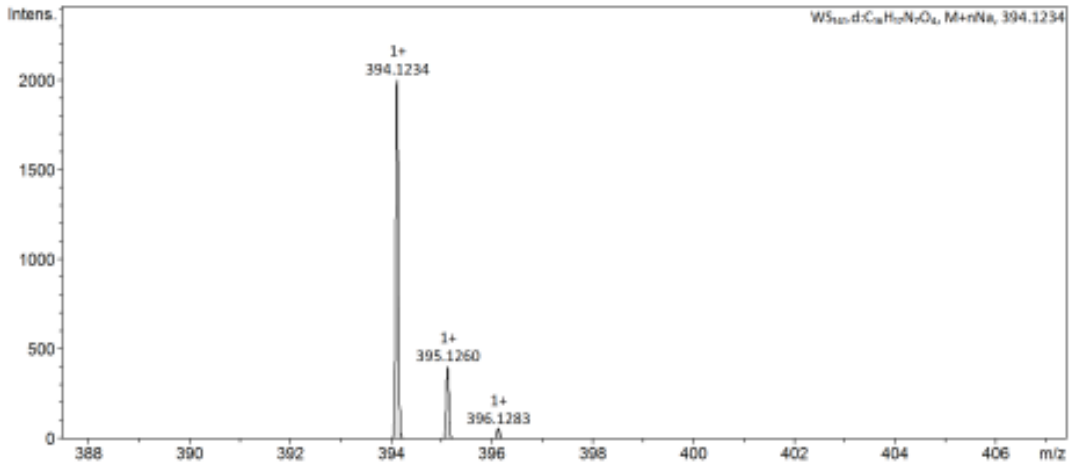

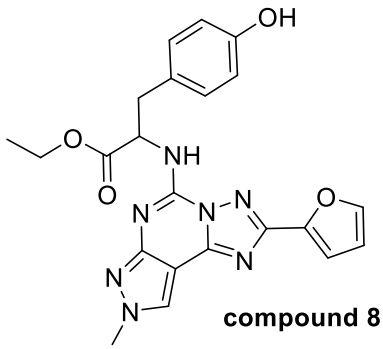
OH
O
O
NH
N
N
N
N
N
O

compound 8

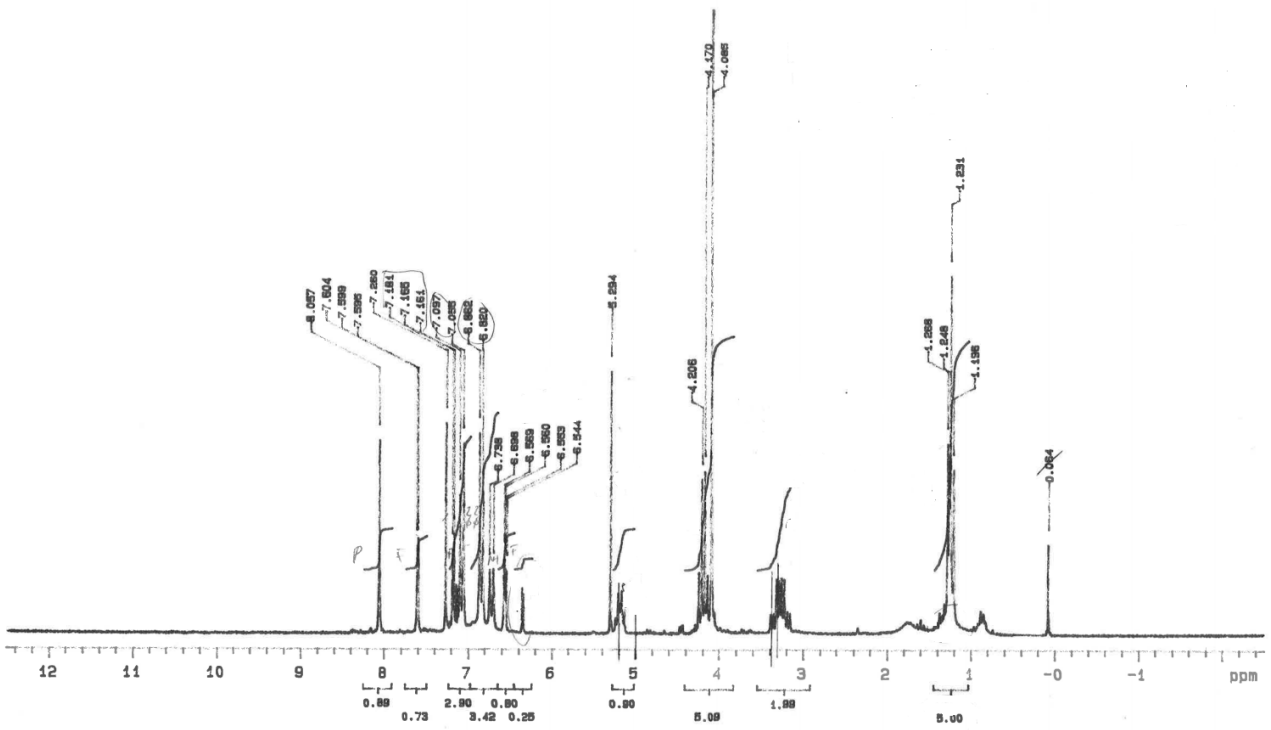
12
11
10
9
8
7
6
5
4
3
2
1
-0
-1
ppm
0.89
0.73
2.90
0.80
3.42
0.25
0.90
5.09
1.99
5.00

Display Report

Analysis Info

Analysis Name	D:\Data\Prato\26.02.20\WS143.d	Acquisition Date	2/26/2020 12:00:32 PM
Method	Leu-Enk.m	Operator	BDAL@DE
Sample Name		Instrument	micrOTOF-Q 8228888.00052
Comment			

Acquisition Parameter

Source Type	ESI	Ion Polarity	Positive	Set Nebulizer	0.4 Bar
Focus	Not active	Set Capillary	4500 V	Set Dry Heater	200 °C
Scan Begin	50 m/z	Set End Plate Offset	-500 V	Set Dry Gas	4.0 l/min
Scan End	1000 m/z	Set Collision Cell RF	350.0 Vpp	Set Divert Valve	Source

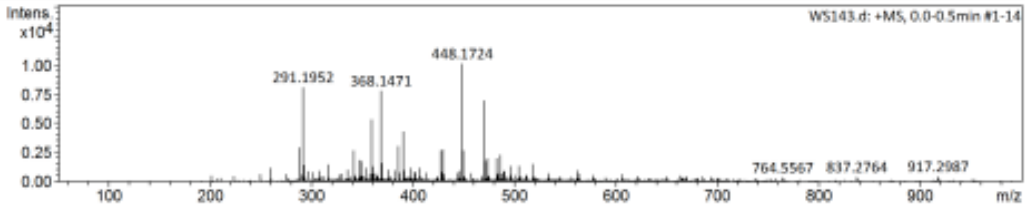

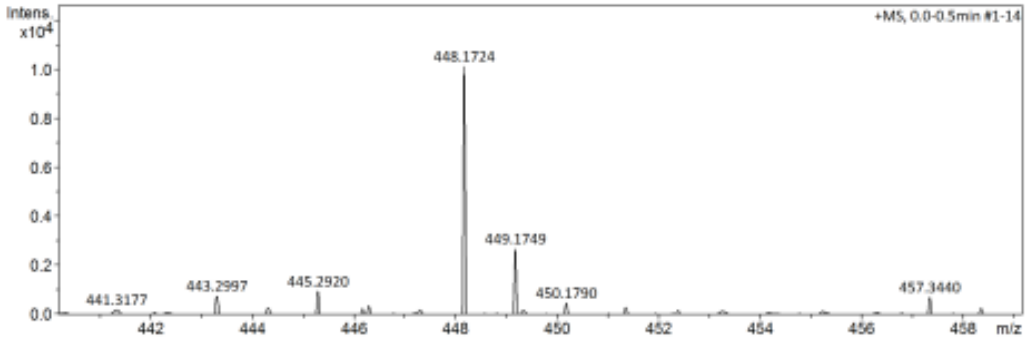

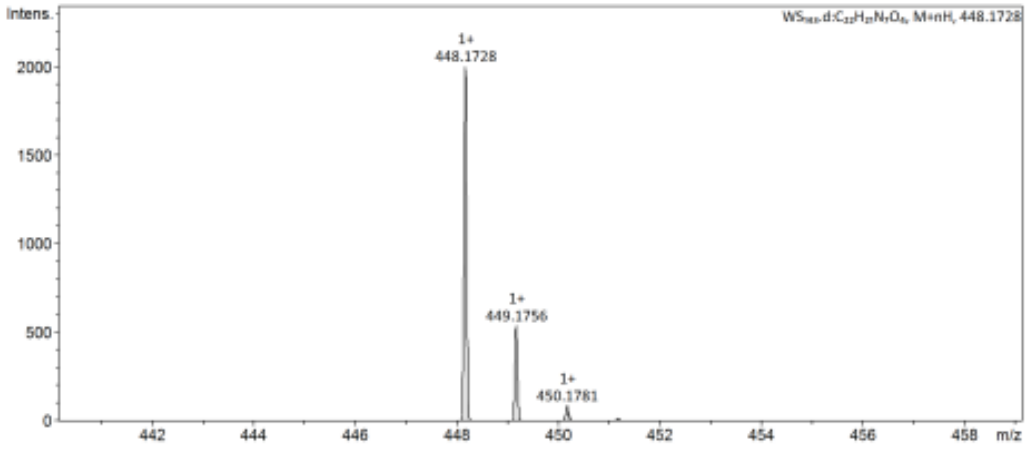

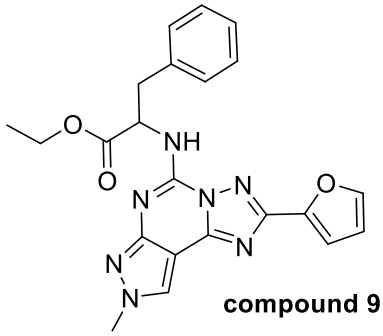
O
NH
O
N
N
N
N
N
O
N
N

compound 9

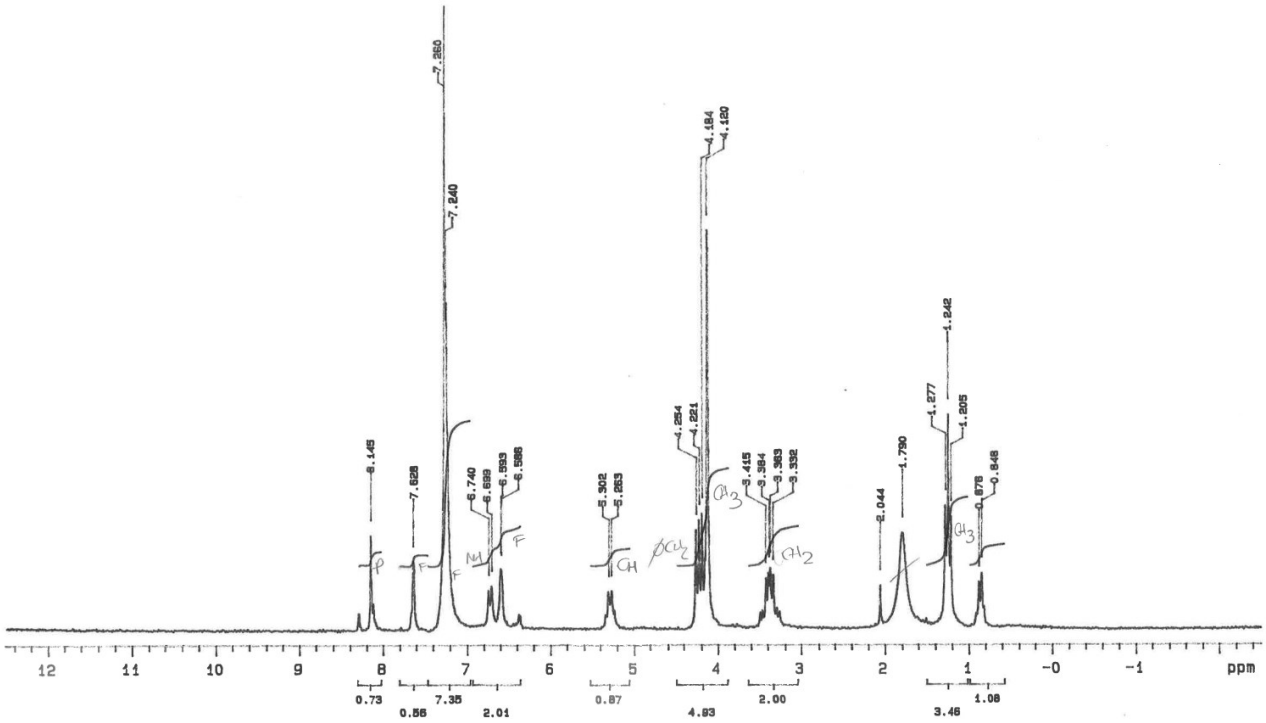
8.145
7.628
7.260
7.240
6.740
6.699
6.593
6.588
5.302
5.283
4.254
4.221
4.184
4.120
3.415
3.384
3.363
3.332
2.044
1.790
1.842
1.277
1.205
0.878
0.848
12
11
10
9
8
7
6
5
4
3
2
1
-0
-1
ppm
0.73
0.56
7.35
2.01
0.87
4.83
2.00
3.46
1.08

Display Report

Analysis Info

Analysis Name	D:\Data\Prato\26.02.20\WS144.d	Acquisition Date	2/26/2020 12:16:58 PM
Method	Leu-Enk.m	Operator	BDAL@DE
Sample Name		Instrument	micrOTOF-Q 8228888.00052
Comment			

Acquisition Parameter

Source Type	ESI	Ion Polarity	Positive	Set Nebulizer	0.4 Bar
Focus	Not active	Set Capillary	4500 V	Set Dry Heater	200 °C
Scan Begin	50 m/z	Set End Plate Offset	-500 V	Set Dry Gas	4.0 l/min
Scan End	1000 m/z	Set Collision Cell RF	350.0 Vpp	Set Divert Valve	Source

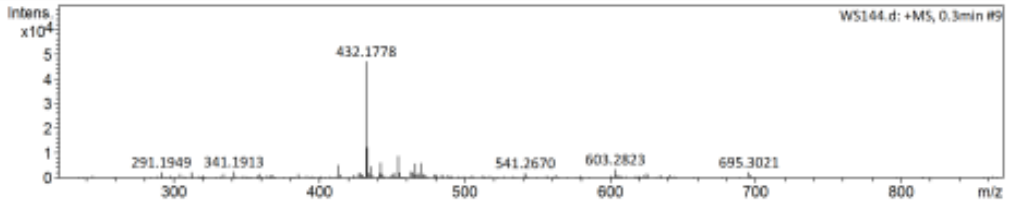

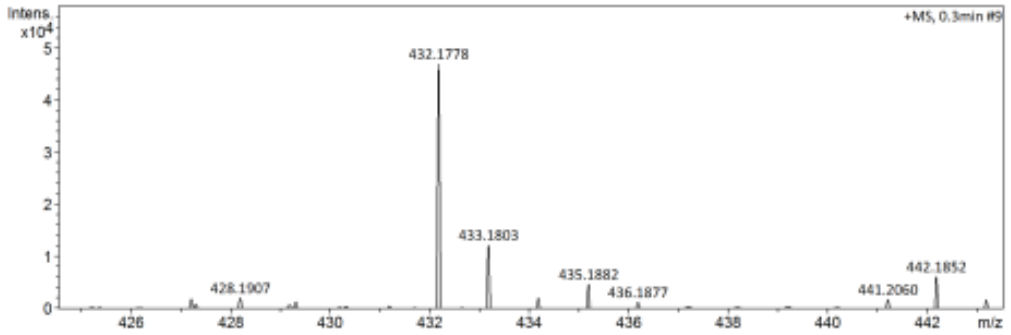

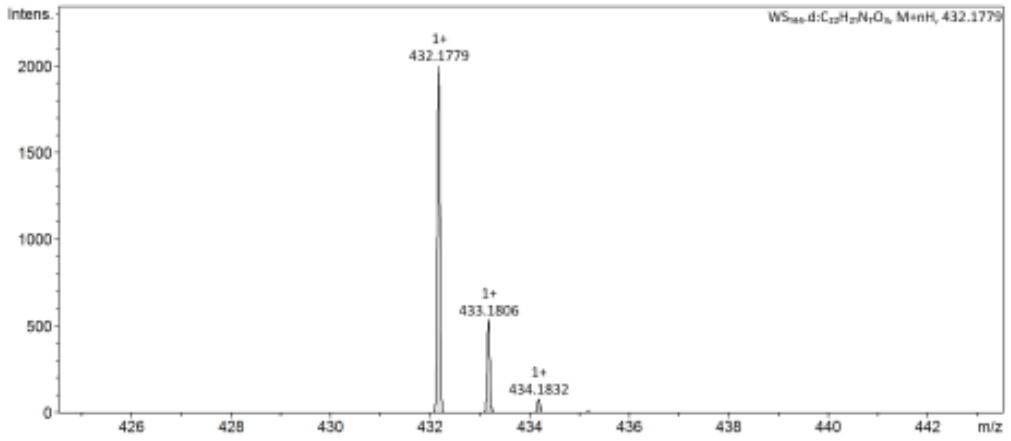

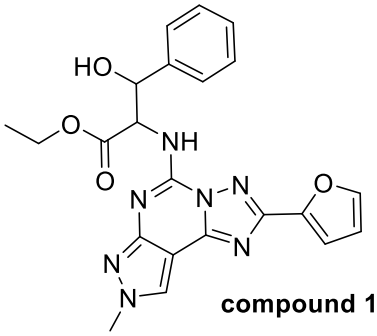

compound 10

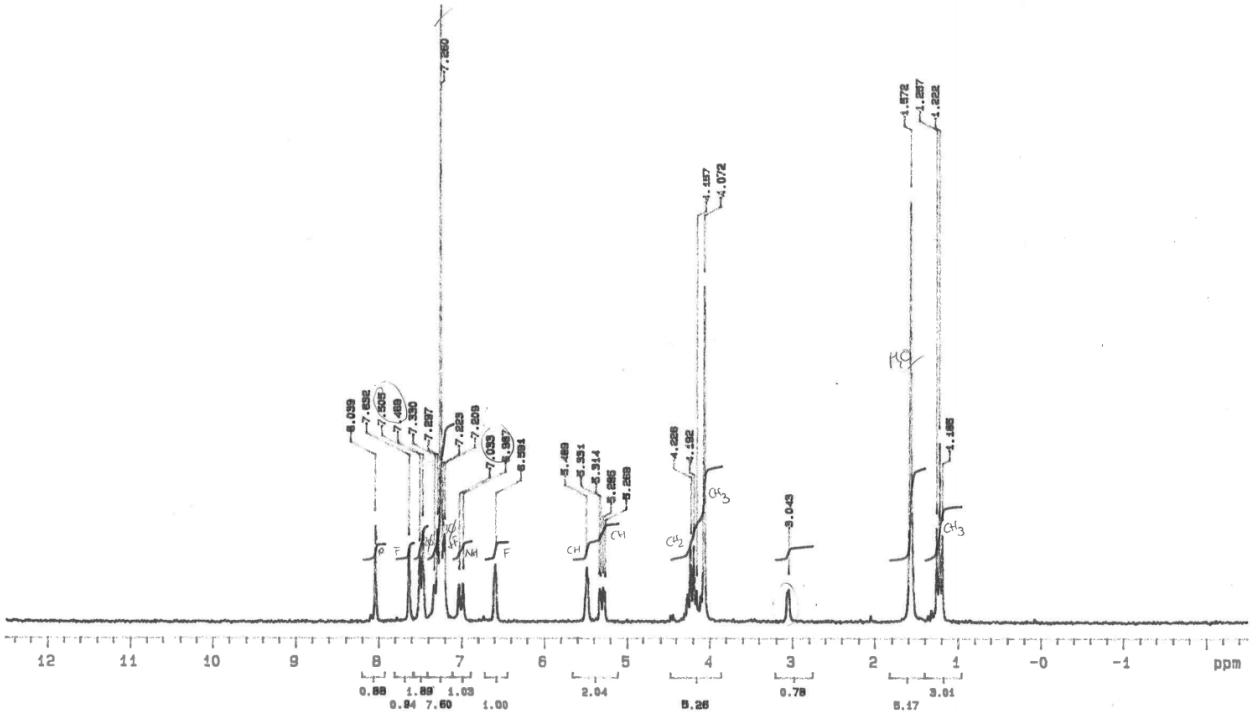

Display Report

Analysis Info

Analysis Name	D:\Data\Prato\26.02.20\WS145.d	Acquisition Date	2/26/2020 12:23:26 PM
Method	Leu-Enk.m	Operator	BDAL@DE
Sample Name		Instrument	micrOTOF-Q 8228888.00052
Comment			

Acquisition Parameter

Source Type	ESI	Ion Polarity	Positive	Set Nebulizer	0.4 Bar
Focus	Not active	Set Capillary	4500 V	Set Dry Heater	200 °C
Scan Begin	50 m/z	Set End Plate Offset	-500 V	Set Dry Gas	4.0 l/min
Scan End	1000 m/z	Set Collision Cell RF	350.0 Vpp	Set Divert Valve	Source

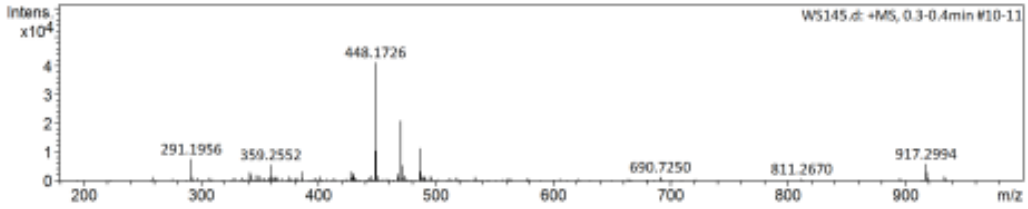

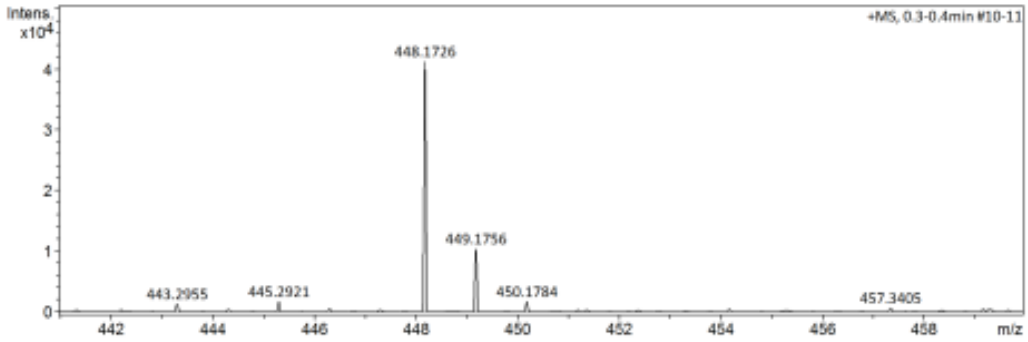

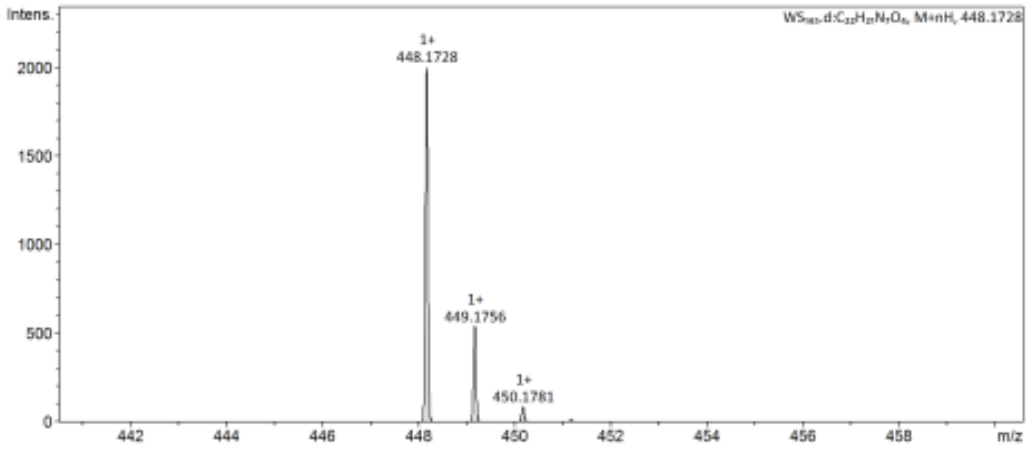

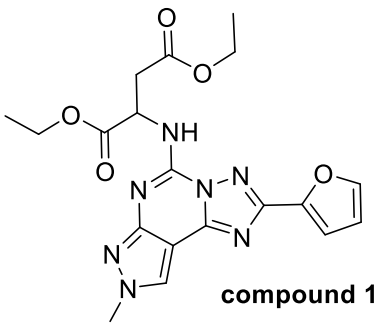

compound 11

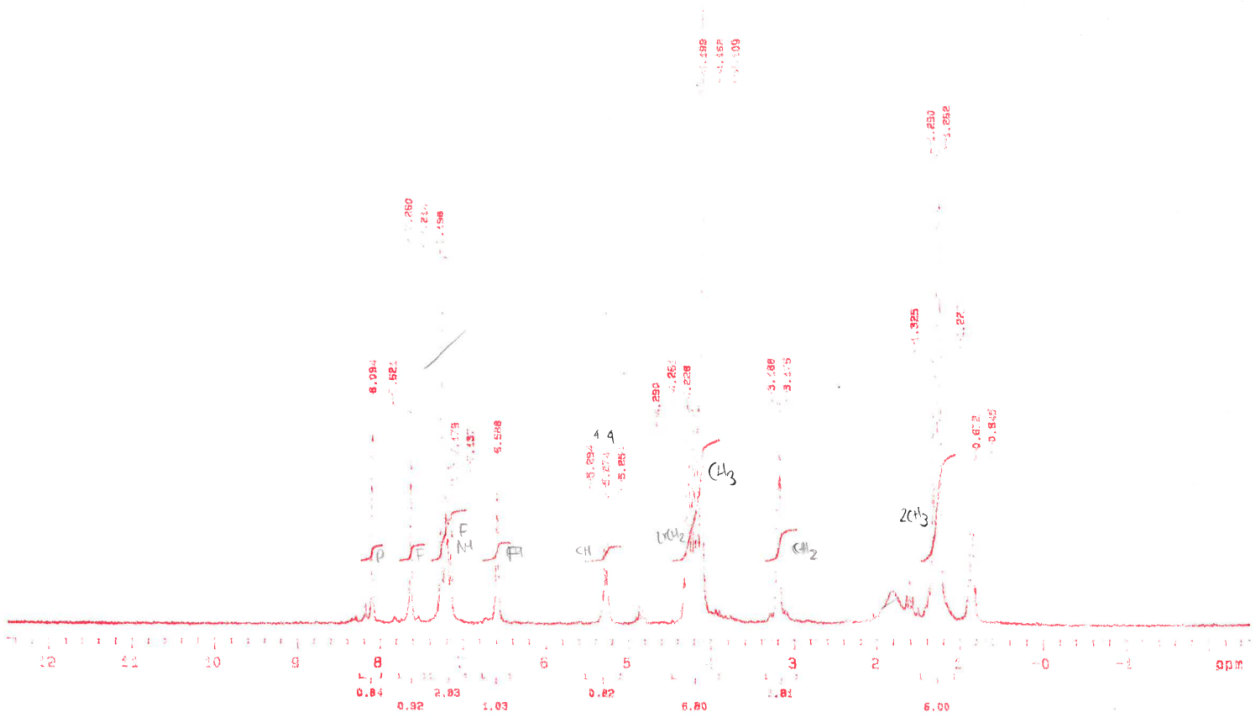

Display Report

Analysis Info

Analysis Name	D:\Data\Prato\26.02.20\WS146.d	Acquisition Date	2/26/2020 12:31:02 PM
Method	Leu-Enk.m	Operator	BDAL@DE
Sample Name		Instrument	micrOTOF-Q 8228888.00052
Comment			

Acquisition Parameter

Source Type	ESI	Ion Polarity	Positive	Set Nebulizer	0.4 Bar
Focus	Not active	Set Capillary	4500 V	Set Dry Heater	200 °C
Scan Begin	50 m/z	Set End Plate Offset	-500 V	Set Dry Gas	4.0 l/min
Scan End	1000 m/z	Set Collision Cell RF	350.0 Vpp	Set Divert Valve	Source

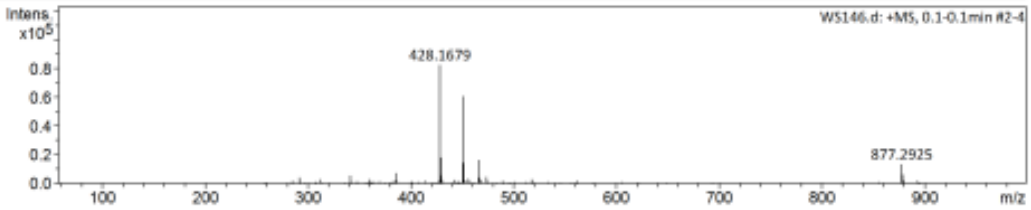

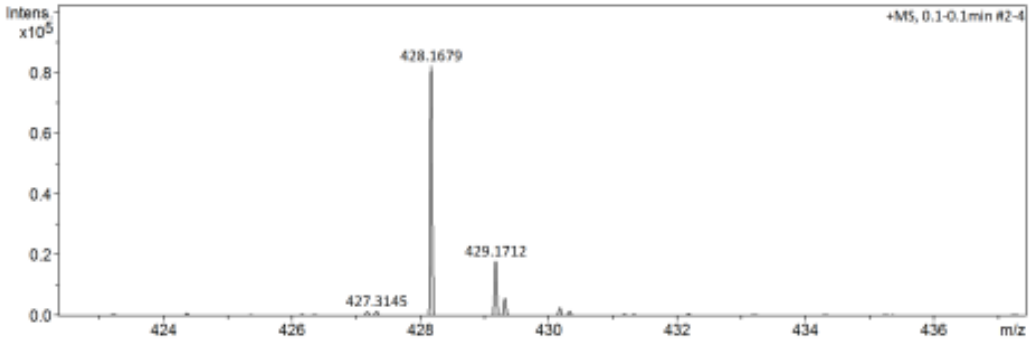

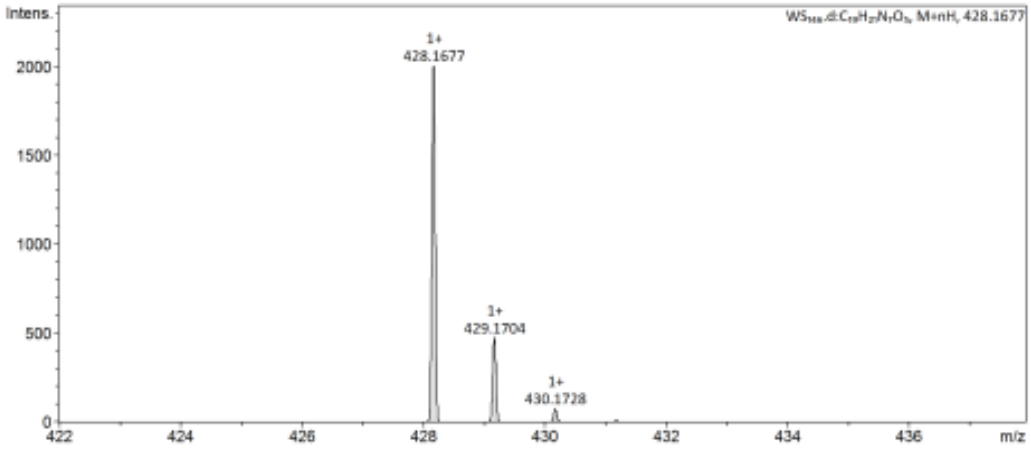

Display Report

Analysis Info

Analysis Name	D:\Data\Prato\26.02.20\WS146.d	Acquisition Date	2/26/2020 12:31:02 PM
Method	Leu-Enk.m	Operator	BDAL@DE
Sample Name		Instrument	micrOTOF-Q 8228888.00052
Comment			

Acquisition Parameter

Source Type	ESI	Ion Polarity	Positive	Set Nebulizer	0.4 Bar
Focus	Not active	Set Capillary	4500 V	Set Dry Heater	200 °C
Scan Begin	50 m/z	Set End Plate Offset	-500 V	Set Dry Gas	4.0 l/min
Scan End	1000 m/z	Set Collision Cell RF	350.0 Vpp	Set Divert Valve	Source

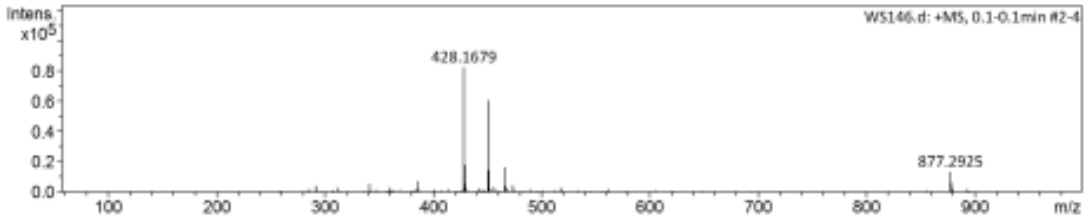

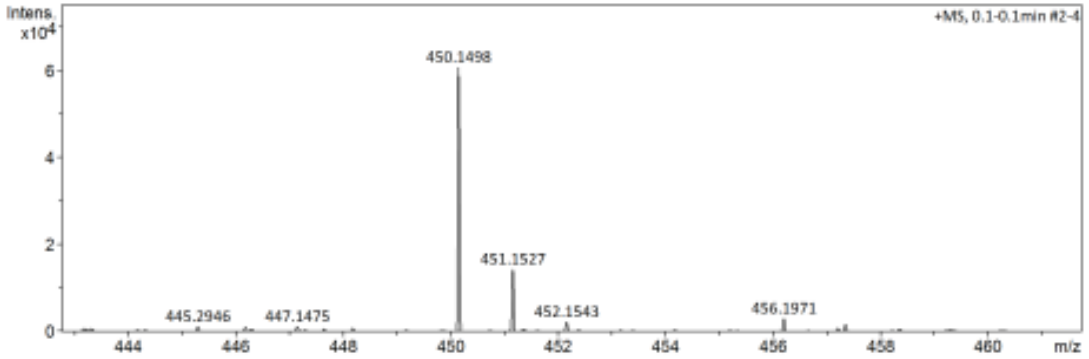

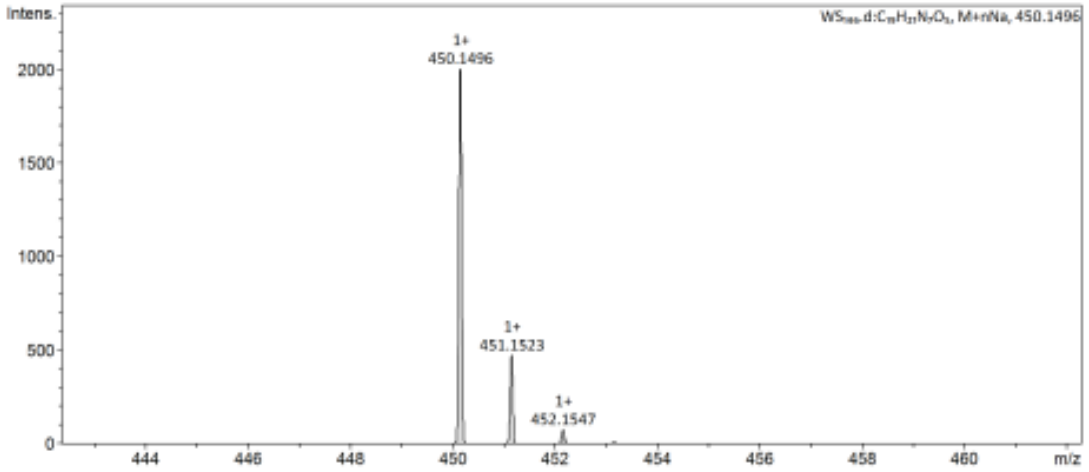

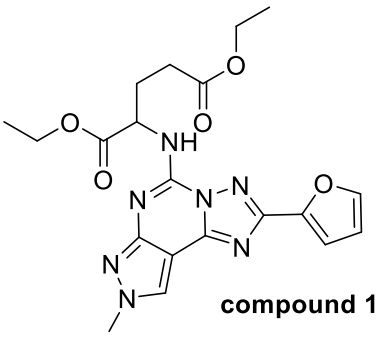

compound 12

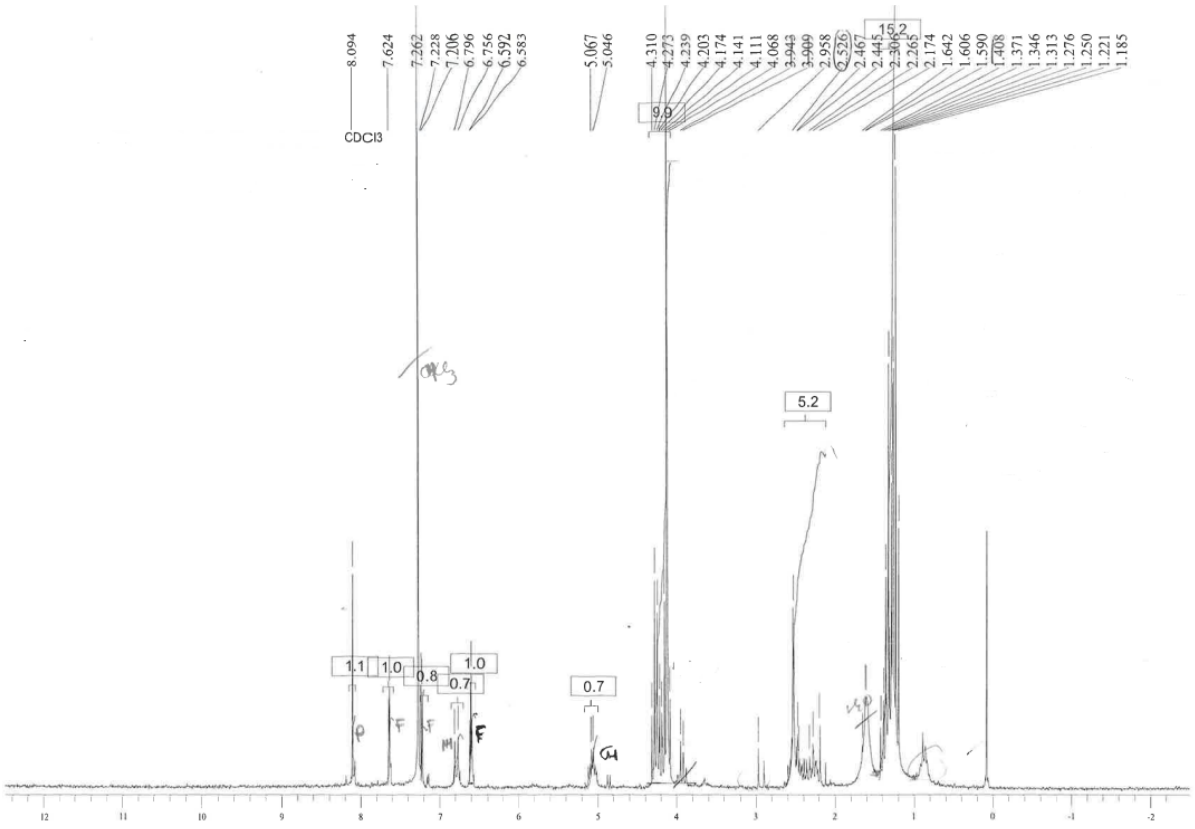
8.094
7.624
7.262
7.228
7.206
6.796
6.756
6.592
6.583
5.067
5.046
4.310
4.273
4.239
4.203
4.174
4.141
4.111
4.068
3.943
3.909
2.958
2.526
2.467
2.445
2.306
2.265
2.174
1.642
1.606
1.590
1.408
1.371
1.346
1.313
1.276
1.250
1.221
1.185
CDCl3
15.2
9.0
5.2
1.1
1.0
0.8
0.7
1.0
0.7

Display Report

Analysis Info

Analysis Name	D:\Data\Prato\26.02.20\WS147.d	Acquisition Date	2/26/2020 12:08:28 PM
Method	Leu-Enk.m	Operator	BDAL@DE
Sample Name		Instrument	micrOTOF-Q 8228688.00052
Comment			

Acquisition Parameter

Source Type	ESI	Ion Polarity	Positive	Set Nebulizer	0.4 Bar
Focus	Not active	Set Capillary	4500 V	Set Dry Heater	200 °C
Scan Begin	50 m/z	Set End Plate Offset	-500 V	Set Dry Gas	4.0 l/min
Scan End	1000 m/z	Set Collision Cell RF	350.0 Vpp	Set Divert Valve	Source

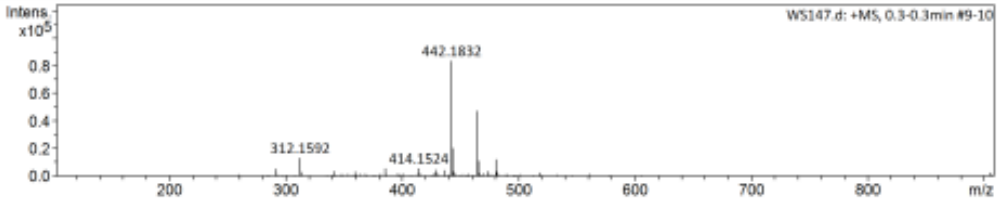

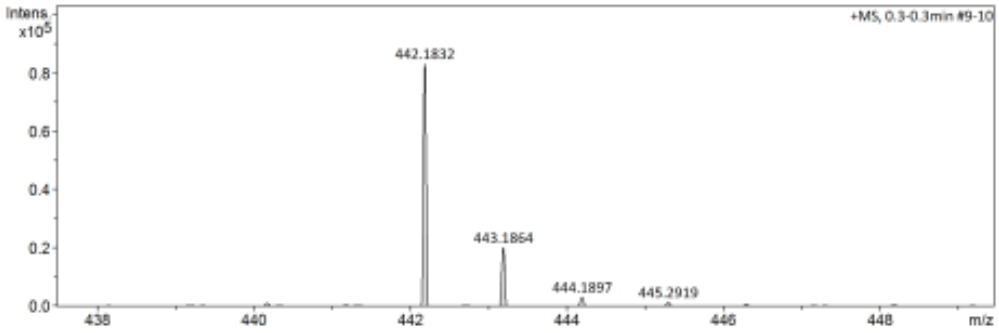

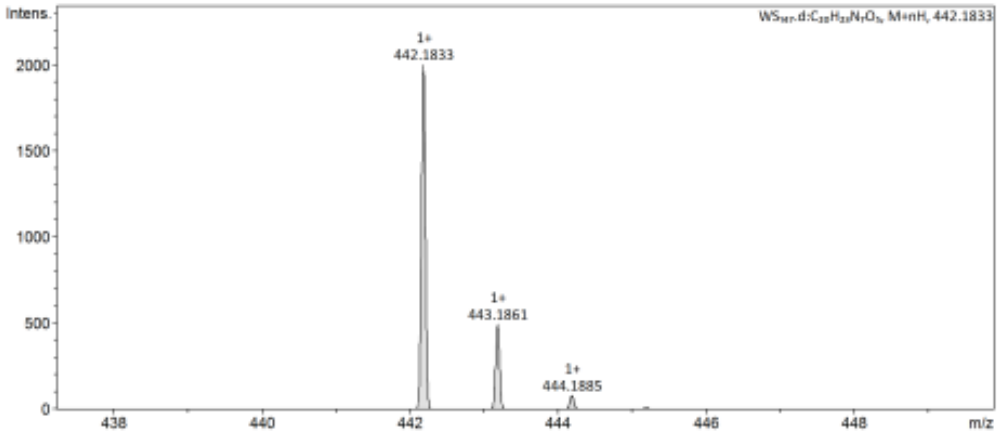

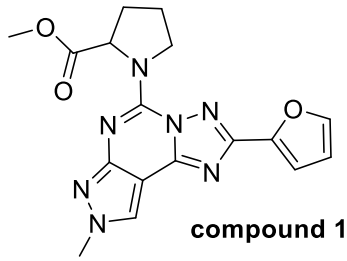

compound 13

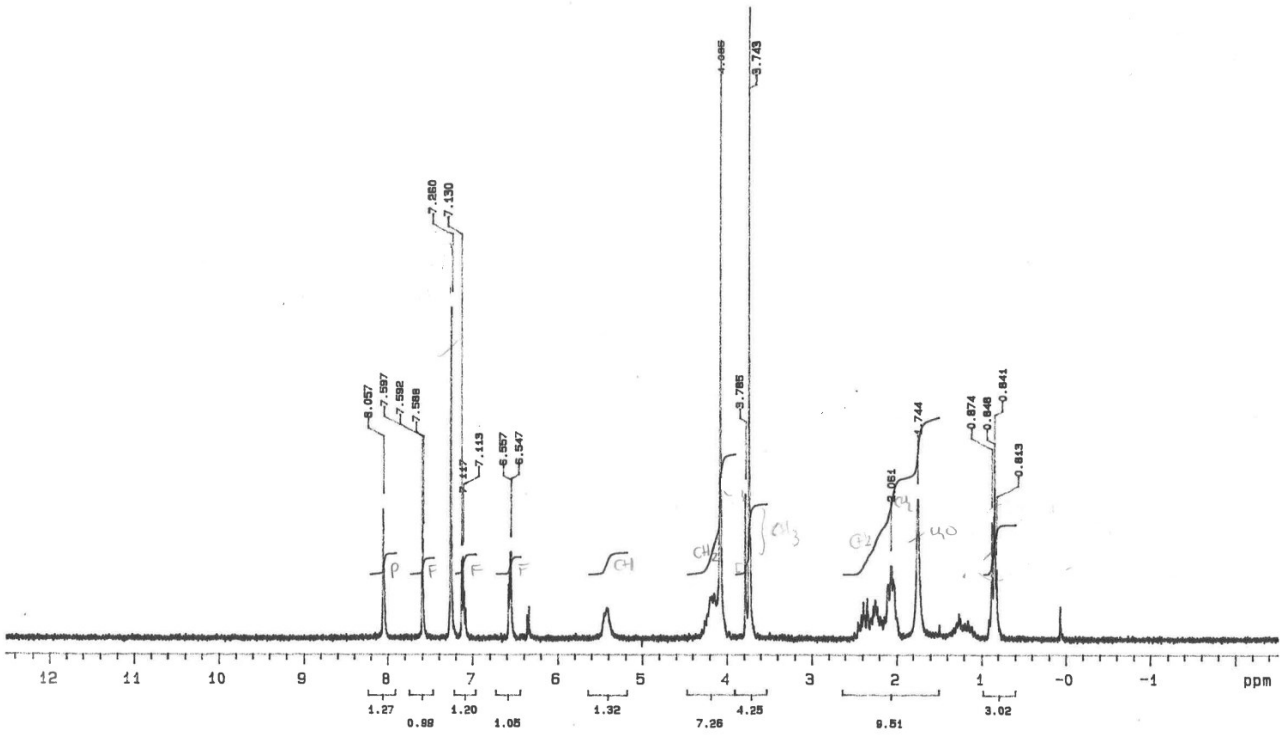
8.057
7.597
7.592
7.588
7.360
7.130
7.117
7.113
6.557
6.547
4.065
3.743
3.785
4.061
4.744
0.874
0.848
0.841
0.813
12
11
10
9
8
7
6
5
4
3
2
1
-0
-1
ppm
1.27
0.99
1.20
1.05
1.32
7.26
4.25
9.51
3.02

Display Report

Analysis Info

Analysis Name	D:\Data\Prato\26.02.20\WS142.d	Acquisition Date	2/26/2020 11:51:36 AM
Method	Leu-Enk.m	Operator	BDAL@DE
Sample Name		Instrument	micrOTOF-Q 8228888.00052
Comment			

Acquisition Parameter

Source Type	ESI	Ion Polarity	Positive	Set Nebulizer	0.4 Bar
Focus	Not active	Set Capillary	4500 V	Set Dry Heater	200 °C
Scan Begin	50 m/z	Set End Plate Offset	-500 V	Set Dry Gas	4.0 l/min
Scan End	1000 m/z	Set Collision Cell RF	350.0 Vpp	Set Divert Valve	Source

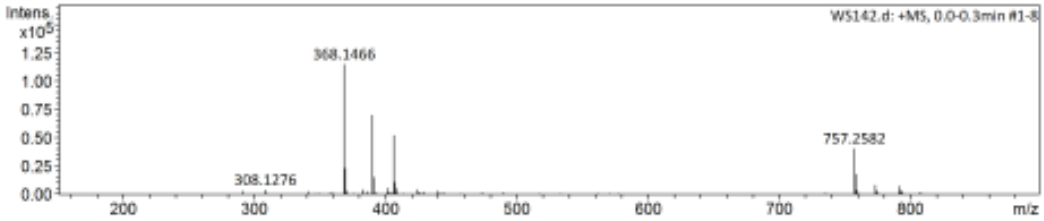

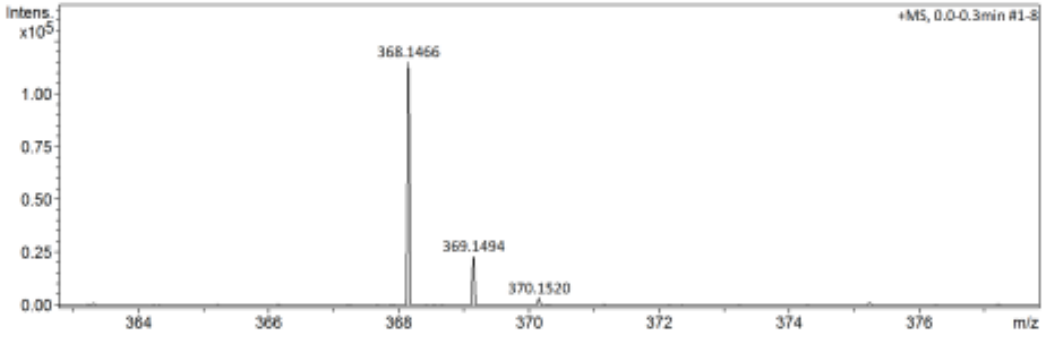

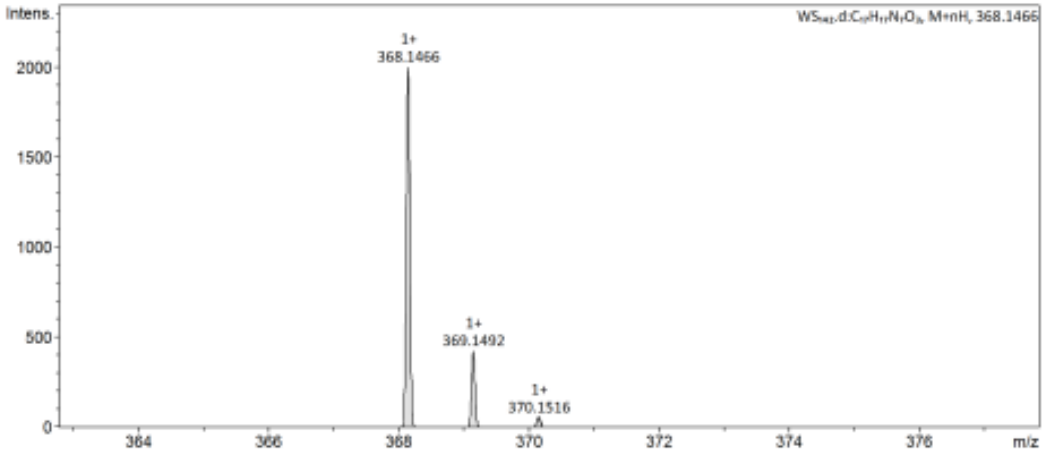

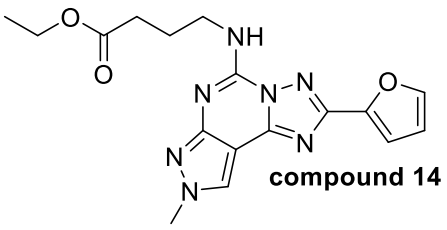
O
O
NH
N
N
N
N
N
O
N

compound 14

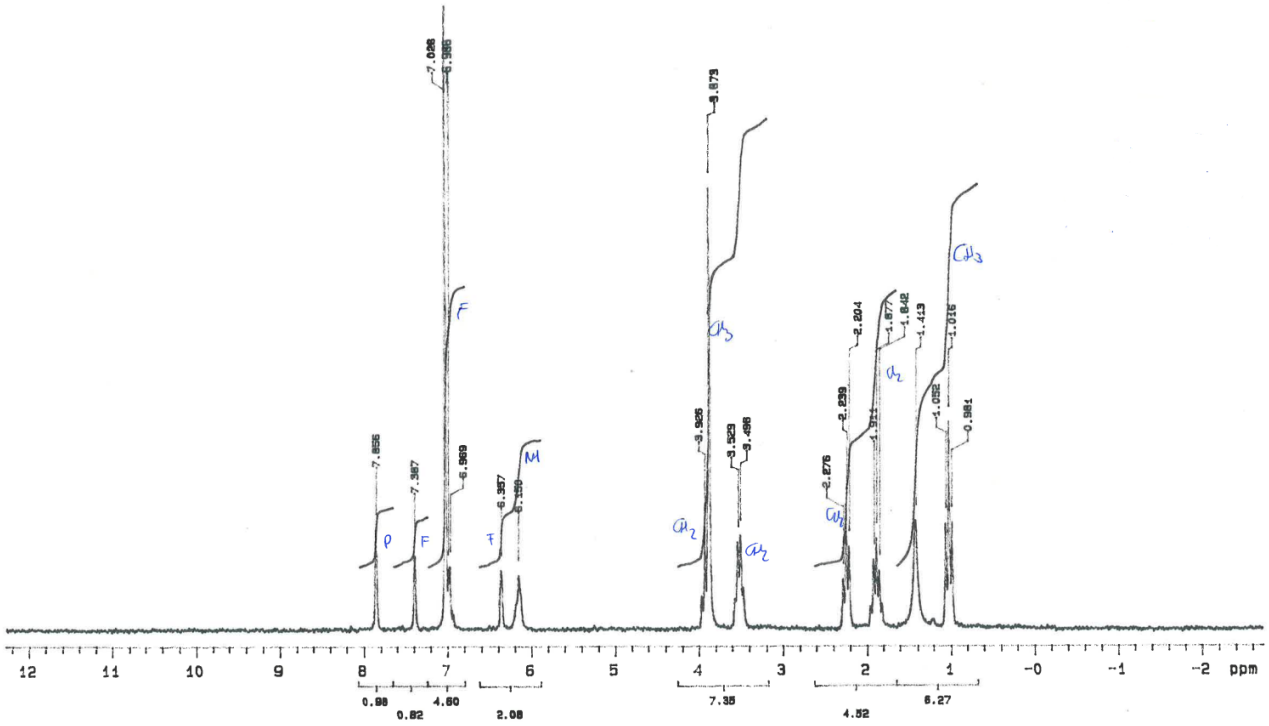
12
11
10
9
8
7
6
5
4
3
2
1
-0
-1
-2
ppm
0.98
4.80
0.82
2.08
7.35
4.52
6.27

Display Report

Analysis Info

Analysis Name	D:\Data\Prato\26.02.20\WS106.d	Acquisition Date	2/26/2020 10:48:51 AM
Method	Leu-Enk.m	Operator	BDAL@DE
Sample Name		Instrument	micrOTOF-Q 8228888.00052
Comment			

Acquisition Parameter

Source Type	ESI	Ion Polarity	Positive	Set Nebulizer	0.4 Bar
Focus	Not active	Set Capillary	4500 V	Set Dry Heater	200 °C
Scan Begin	50 m/z	Set End Plate Offset	-500 V	Set Dry Gas	4.0 l/min
Scan End	1000 m/z	Set Collision Cell RF	350.0 Vpp	Set Divert Valve	Source